Geochronology, 6, 175–198, 2024
https://doi.org/10.5194/gchron-6-175-2024


# A new method for amino acid geochronology of the shell of the bivalve mollusc *Arctica islandica*

**Martina L. G. Conti[1], Paul G. Butler[2], David J. Reynolds[2], Tamara Trofimova[2], James D. Scourse[2], and Kirsty E. H. Penkman[1]**

[1]Department of Chemistry, University of York, York, YO10 5DD, United Kingdom
[2]Centre For Geography and Environmental Science, University of Exeter, Penryn, United Kingdom

**Correspondence:** Martina L. G. Conti (martina.conti@york.ac.uk)

Received: 31 October 2023 – Discussion started: 15 November 2023
Accepted: 18 March 2024 – Published: 23 May 2024

**Abstract.** The bivalve mollusc *Arctica islandica* can live for hundreds of years, and its shell has provided a valuable resource for sclerochronological studies and geochemical analyses for understanding palaeoenvironmental change. Shell specimens recovered from the seabed need to be dated in order to aid sample selection, but existing methods using radiocarbon dating or cross-dating are both costly and time-consuming. We have investigated amino acid geochronology (AAG) as a potential alternative means of providing a less costly and more efficient range-finding method. In order to do this, we have investigated the complex microstructure of the shells, as this may influence the application of AAG. Each of the three microstructural layers of *A. islandica* have been isolated and their protein degradation examined (amino acid concentration, composition, racemization, and peptide bond hydrolysis). The intra-crystalline protein fraction was successfully extracted following oxidation treatment for 48 h, and high-temperature experiments at 140 °C established coherent breakdown patterns in all three layers, but the inner portion of the outer shell layer (iOSL) was the most appropriate component due to practicalities. Sampling of the iOSL layer in Holocene shells from early and late ontogeny (over 100–400 years) showed that the resolution of AAG is too low in *A. islandica* for within-shell age resolution. However, analysis of 52 subfossil samples confirmed that this approach could be used to establish a relative geochronology for this biomineral throughout the whole of the Quaternary. In the late Holocene the temporal resolution is ∼ 1500–2000 years. Relative dating of 160 dredged shells of unknown age was narrowed down using AAG as a range finder, showing that a collection of shells from Iceland and the North Sea covered the middle Holocene, late Holocene, later and post-medieval (1171–1713 CE), and modern day. This study confirms the value of *A. islandica* as a reliable material for range finding and for dating Quaternary deposits.

## 1 Introduction

*Arctica islandica* (ocean quahog) is a bivalve mollusc that inhabits the continental shelf seas across the North Atlantic region (MarLIN database). It presently lives across subpolar latitudes of the North Atlantic region of Europe from the English Channel to the White Sea and in North America from Virginia to Nova Scotia (MarLIN database; Schöne, 2013). Its Quaternary subfossil shells are also found in ancient sediments in northern Europe and in the Mediterranean Sea (Malatesta and Zarlenga, 1986; Eyles et al., 1994; Crippa et al., 2019). *Arctica islandica* has been routinely used for palaeoclimate and palaeoceanographic studies due its exceptionally long life (> 500 years' maximum longevity; Butler et al., 2013) and its capability to capture climatological changes within its periodic accretions (i.e. growth lines; Witbaard et al., 1997; Schöne et al., 2005; Schöne, 2013; Butler et al., 2013; Reynolds et al., 2016; Estrella-Martínez et al., 2019). The study of annual and subannual band growth variability within the calcium carbonate shells, termed sclerochronology (Fig. 1), provides detailed high-resolution palaeoclimatology data spanning decades to multiple centuries (Schöne et al., 2004; Schöne and Fiebig, 2009; Dunca et al., 2009; Butler et al., 2009, 2013; Wanamaker

et al., 2012; Reynolds et al., 2016; Trofimova et al., 2018; Estrella-Martinez et al., 2019; Brosset et al., 2022).

Developing sclerochronological records requires visual and statistical cross-matching across numerous samples; this endeavour can be hugely time-consuming and therefore needs to be targeted appropriately, especially when dead-collected samples are of unknown age. Dating of the specimens is essential to develop accurate sclerochronological records: radiocarbon dating can be a very precise technique for late Quaternary marine shells (back to 40 000–55 000 years). However, this is not always economically viable (Hajdas et al., 2021), especially for a large number of samples, as accurate correction for the marine reservoir effect is required, and the dating uncertainty can be a few hundred years (Alves et al., 2018). One possible alternative is amino acid geochronology (AAG), a relative-age technique that is comparatively fast and inexpensive. AAG is applicable to mollusc shell deposits spanning the Quaternary period (e.g. Sejrup and Haugen, 1994; Davies et al., 2009; Ortiz et al., 2009, 2015; Penkman, 2010; Demarchi et al., 2013a, b; Bridgland et al., 2013), and it can have high precision and resolution in tropical corals (Hendy et al., 2012).

AAG dating of biominerals is based on the natural degradation of proteins to determine age. The main processes are racemization and epimerization, both leading to an increase in amino acid D/L; peptide bond hydrolysis; and amino acid decomposition (Hare and Mitterer, 1969). When organisms die, or when there is no more tissue turnover, these degradation reactions occur in tandem. The inter-crystalline fraction of biominerals (Gries et al., 2009), the protein which forms a matrix between the crystallites, is potentially more susceptible to external contamination or leaching and can compromise the reliability of AAG in some biominerals (Sykes et al., 1995; Penkman et al., 2008; Ortiz et al., 2015). In some materials, a small fraction of the protein is contained within the interstitial voids of the crystal structure and can be isolated with an oxidizing pre-treatment; this is defined as the intra-crystalline (IcP) fraction (Towe and Thompson, 1972; Sykes et al., 1995; Penkman et al., 2008; Gries et al., 2009). The IcP can be isolated with oxidation using NaOCl (or $H_2O_2$ in some cases), and its stability against external contamination and leaching means that, in some biominerals, it effectively operates as a closed system. The isolation of closed-system IcP has provided reliable chronological information in some gastropods (Penkman et al., 2008; Ortiz et al., 2015; Demarchi et al., 2013a, b; Bridgland et al., 2013), ostracods (Ortiz et al., 2013), corals (Hendy et al., 2012; Tomiak et al., 2013, 2016), eggshell (Brooks et al., 1990; Crisp et al., 2013), enamel (Dickinson et al., 2019; Baleka et al., 2021), and foraminifera (Wheeler et al., 2021) but not in all biominerals (e.g. Orem and Kaufman, 2011; Torres et al., 2013; Demarchi et al., 2015).

A further complication for AAG of bivalve shells is that the different microstructural layers in bivalves are likely to be composed of different proteins and therefore may degrade differently. The *A. islandica* shell comprises a periostracum and three aragonitic layers of differing crystal microstructure (Schöne, 2013): a homogeneous granular structure in the outer portion of the outer shell layer (oOSL), a cross-acicular structure for the inner portion of the outer shell layer (iOSL), and a cross-lamellar-to-cross-acicular structure for the inner shell layer (ISL; Fig. 1; Dunca et al., 2009; Schöne, 2013; Milano et al., 2017).

*Arctica islandica*, *Glycymeris glycymeris*, *Callista chione*, and *Entemnotrochus adansonianus* have shown distinct racemization and epimerization rates which depend on the microstructural layer analysed (Haugen and Sejrup, 1990, 1992; Sejrup and Haugen, 1994; Goodfriend et al., 1995, 1997; Torres et al., 2013; Demarchi et al., 2015). Early studies without chemical oxidation on *A. islandica* (i.e. combining both the inter- and any intra-crystalline fraction) showed different epimerization rates, AA concentrations, and composition between the inner and outer layers (Haugen and Sejrup, 1990, 1992; Sejrup and Haugen, 1994). Intra-shell variability was also high, hypothesized to be due to a microorganism attack of the protein during the early stages of diagenesis, external contamination, and/or leaching through micropores (Sejrup and Haugen, 1994; Kosnik and Kaufman, 2008). A study on the use of D/L for ontogenetic studies of unbleached shells revealed Asp D/L (aspartic acid as referred to by Goodfriend and Weidman, 2001) values higher in the umbo growth lines (laid down when the shells are young) compared to the rim growth lines (deposited when the shell is old; Goodfriend and Weidman, 2001). A difference in AA composition between early and late ontogeny was also observed, indicating the need for sampling standardization; the recommendation was to sample shells from band year 20 in the outer shell layer (Goodfriend and Weidman, 2001). Asx D/L values (Asx indicating aspartic acid and asparagine, which cannot be analytically distinguished due to irreversible deamination) in unbleached *A. islandica* shells collected between 1982 and 1994 were shown to increase with age over a 154-year chronology, highlighting that AAG can potentially help in dating sclerochronologies (Marchitto et al., 2000).

Given the variability observed in unbleached *A. islandica* shell AA data, a way forward is to test for the presence of any IcP in *A. islandica* shells and whether it forms a closed system for individual microstructures (e.g. Torres et al., 2013; Demarchi et al., 2013a, b, 2015; Baldreki et al., 2024). The use of IcP in AAG has not been fully investigated in *A. islandica* (Sykes et al., 1995), and there is a variety in the sampling strategy for specific microstructural layers (Haugen and Sejrup, 1990, 1992; Sejrup and Haugen, 1994; Marchitto et al., 2000; Goodfriend and Weidman, 2001). If it is possible to isolate an intra-crystalline fraction that exhibits closed-system behaviour from any of the layers in *A. islandica* shells, an IcP approach may be able to reduce the intra-shell viability and increase accuracy.

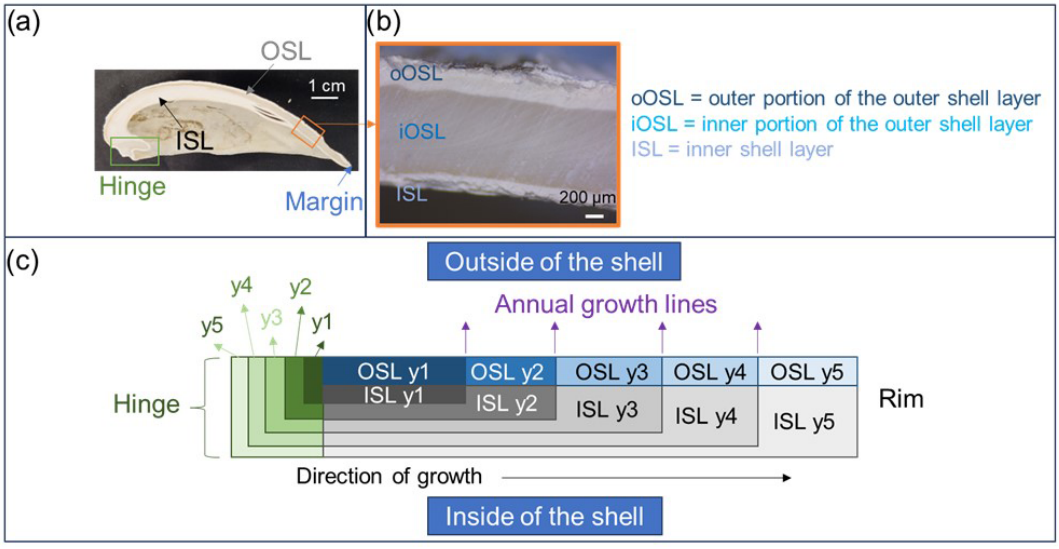


**Figure 1.** **(a)** Cross-section of *Arctica islandica* showing **(b)** the inner shell layer (ISL), inner portion of the outer shell layer (iOSL), and outer portion of the outer shell layer (oOSL). **(c)** Simplified schematics of the growth of ISL and OSL and hinge ("y" indicates the year of growth).

### 1.1 Aims

We present here a new method for the preparation of aragonitic *A. islandica* shells for AAG. To develop this methodology, the following experiments were conducted:

- optimization of the sampling method and isolation of the three microstructural layers (Sect. 2.2)
- assessment of aragonitic mineral diagenesis via X-ray diffraction (XRD) analysis (Sect. 3.1)
- testing for the existence of an intra-crystalline protein fraction via oxidation experiments (Sect. 3.2)
- testing for closed-system behaviour of *A. islandica* through controlled high-temperature decomposition experiments and assessment of the amino acid degradation patterns (Sect. 3.3)
- assessment of any change in amino acid composition and D/L values with ontogeny (Sect. 3.4)
- optimized method and recommendations for IcPD analysis of *A. islandica* (Sect. 3.5)
- analysis of multiple independently dated subfossil shells to develop an initial AAG framework for *A. islandica* in the North Atlantic Ocean (Sect. 3.6)
- age range finding of undated shells collected during research cruise DY150 of RRS *Discovery* in spring 2022 (Sect. 3.7).

## 2 Materials and methods

### 2.1 *A. islandica* specimens

In total, 19 *A. islandica* subfossil samples from the North Sea and Iceland were obtained for the bleaching and high-temperature experiments, ontogenetic trends, and initial framework; these spanned in age from modern to ∼ 2.1–2.2 Ma and were independently dated with radiocarbon ($^{14}$C), AAG on other biominerals (see Table 1 for details; Fig. 2), and sclerochronological cross-dating (S; Table 1). In addition, 160 *A. islandica* shells of unknown age, incorporating samples from both the North Sea and the North Icelandic shelf, were analysed for range finding (Sect. 3.7; Fig. 2).

### 2.2 Sampling

Each individual shell was sectioned from the umbo to the margin with an IsoMet 1000 precision cutter. After slicing, the shells were sonicated in deionized water (18.2 MΩ cm$^{-1}$) until no residue was observed (3 min, 2–3 washes). After air drying, the periostracum (if present) was removed by drilling with an abrasive rotary burr on a handheld rotary tool (Dremel drill). Each layer (oOSL, iOSL, and ISL; Fig. 1) was sampled by drilling using a Dremel drill equipped with a stainless-steel diamond-coated drill bit with a small sphere or cylindrical tip. Following the experiments in Sect. 3.3 and 3.4, the iOSL layer was chosen for building the AAG framework. To check changes in amino acids with ontogeny (e.g. with the biological age of the shell; Sect. 3.4), the iOSL from early and late ontogeny within one shell (Table 1) was sampled: the former near the hinge and the latter close to the

https://doi.org/10.5194/gchron-6-175-2024

**Table 1.** Overview of the *A. islandica* shells analysed in this study: numbers correspond to the location on the map (Fig. 2), and Rf indicates shell locations used in the range-finding study (Sect. 3.7). Methods of dating: AAG is amino acid geochronology, $^{14}C$ is radiocarbon, and S is sclerochronologically cross-dated.

| Sample name | Number of shells and code | Locality | Latitude | Longitude | Estimated age | Independent previous dating | Reference for previous dating | Experiment |
|---|---|---|---|---|---|---|---|---|
| (A) ArBrMod | $n = 1$ n/a | Bridlington Beach, UK | 54°4′ N | 0°11′ W | Modern?[a], beach-collected July 2021 | n/a | n/a | pXRD (Sect. 3.1), framework (Sect. 3.6), range finding (Sect. 3.7) |
| (B) ArPe, ArPe2 | $n = 2$ n/a | North Sea off Peterhead | 58°37′ N | 1°27′ E | Modern, live-collected, trawled at −114 m depth in 2018 | n/a | http://schnecken-und-muscheln.de (last access: 21 November 2022, purchased in 2022) | Bleaching (Sect. 3.2), high temperature (Sect. 3.3), framework (Sect. 3.6), range finding (Sect. 3.7) |
| (C) ArNsM1 | $n = 1$ 0401381R | North Sea | 59°23.10′ N | 0°31.00′ E | 1865–2004 CE | S | Butler et al. (2009) | Ontogenetic trends (Sect. 3.4), framework (Sect. 3.6), range finding (Sect. 3.7) |
| (D) ArNsM2 | $n = 1$ 0401422L | North Sea | 59°23.10′ N | 0°31.00′ E | 1874–2004 CE | S | Butler et al. (2009) | Ontogenetic trends (Sect. 3.4), framework (Sect. 3.6), range finding (Sect. 3.7) |
| (E) ArNsM3 | $n = 1$ 0401423L | North Sea | 59°23.10′ N | 0°31.00′ E | 1908–2004 CE | S | Butler et al. (2009) | Ontogenetic trends (Sect. 3.4), framework (Sect. 3.6), range finding (Sect. 3.7) |
| (F) ArNs0246 | $n = 1$ 0400246 | North Sea | 59°7.5′ N | 0°10.0′ E | 1867–2004 CE | S | Butler et al. (2009) | pXRD (Sect. 3.1), ontogenetic trends (Sect. 3.4), framework (Sect. 3.6), range finding (Sect. 3.7) |
| (G) ArIcP2 | $n = 1$ 061683M | Iceland | 66°31.59′ N | 18°11.74′ W | 1397–1713 CE | S | Butler et al. (2013) | Ontogenetic trends (Sect. 3.4), framework (Sect. 3.6), range finding (Sect. 3.7) |
| (H) ArIcP1 | $n = 1$ 061682M | Iceland | 66°31.59′ N | 18°11.74′ W | 1171–1391 CE | S | Butler et al. (2013) | pXRD (Sect. 3.1), ontogenetic trends (Sect. 3.4), framework (Sect. 3.6), range finding (Sect. 3.7) |
| (I) ArIc617 | $n = 1$ 061617 | Iceland | 66°31.59′ N | 18°11.74′ W | $2841 \pm 33$ $^{14}C$ yr BP 2545–2119 cal yr BP $2\sigma$ | $^{14}C$[b] | n/a | Framework (Sect. 3.6), range finding (Sect. 3.7) |
| (J) ArIc711 | $n = 1$ 061711 | Iceland | 66°31.59′ N | 18°11.74′ W | $2938 \pm 33$ $^{14}C$ yr BP 2678–2292 cal yr BP $2\sigma$ | $^{14}C$[b] | n/a | Framework (Sect. 3.6), range finding (Sect. 3.7) |
| (K) ArIc407 | $n = 1$ 061407 | Iceland | 66°31.59′ N | 18°11.74′ W | $3411 \pm 37$ $^{14}C$ yr BP 3223–2817 cal yr BP $2\sigma$ | $^{14}C$[b] | n/a | Framework (Sect. 3.6), range finding (Sect. 3.7) |
| (L) ArIc746 | $n = 1$ 061746 | Iceland | 66°31.59′ N | 18°11.74′ W | $3535 \pm 36$ $^{14}C$ yr BP 3364–2975 cal yr BP $2\sigma$ | $^{14}C$[b] | n/a | Framework (Sect. 3.6), range finding (Sect. 3.7) |
| (M) ArIc305 | $n = 1$ 061305 | Iceland | 66°31.59′ N | 18°11.74′ W | $4222 \pm 40$ $^{14}C$ yr BP 4257–3826 cal yr BP $2\sigma$ | $^{14}C$[b] | n/a | Framework (Sect. 3.6), range finding (Sect. 3.7) |
| (N) ArNs0658 | $n = 1$ 010658 | Fladen Ground (North Sea) | 58°50′ N | 0°21.35′ W | $7810 \pm 25$ $^{14}C$ yr BP 8340–8100 cal yr BP $2\sigma$ | $^{14}C$ (Marine13 calibration) | Estrella-Martinez (2019) | Framework (Sect. 3.6), range finding (Sect. 3.7) |

**Table 1.** Continued.

| Sample name | Number of shells and code | Locality | Latitude | Longitude | Estimated age | Independent previous dating | Reference for previous dating | Experiment |
|---|---|---|---|---|---|---|---|---|
| (O) ArNsP1 | $n = 1$ 10660 | Fladen Ground (North Sea) | 58°49.52′ N | 0°21.6′ W | $7801 \pm 29$ $^{14}$C yr BP 8330–8070 cal yr BP $2\sigma$ | $^{14}$C (Marine13 calibration) | Estrella-Martinez (2019) | Ontogenetic trends (Sect. 3.4), framework (Sect. 3.6), range finding (Sect. 3.7) |
| (P) ArNsP2 | $n = 1$ 10682 | Fladen Ground (North Sea) | 58°49.52′ N | 0°21.6′ W | $7794 \pm 24$ $^{14}$C yr BP 8320–8060 cal yr BP $2\sigma$ | $^{14}$C (Marine13 calibration) | Estrella-Martinez (2019) | Ontogenetic trends (Sect. 3.4), framework (Sect. 3.6), range finding (Sect. 3.7) |
| (Q) ArNsP3, ArNs0684 | $n = 1$ 10684 | Fladen Ground (North Sea) | 58°49.52′ N | 0°21.6′ W | $7752 \pm 23$ $^{14}$C yr BP 8280–8020 cal yr BP $2\sigma$ | $^{14}$C (Marine13 calibration) | Estrella-Martinez (2019) | pXRD (Sect. 3.1), ontogenetic trends (Sect. 3.4), framework (Sect. 3.6), range finding (Sect. 3.7) |
| (R) ArWey | $n = 1$ n/a | Weybourne Crag, UK | 52°56.55′ N | 1°08.33′ E | Early Pleistocene (2.2–2.1 Ma) | AAG on *Bithynia* opercula and *Nucella*, biostratigraphic evidence | Preece et al. (2020) | pXRD (Sect. 3.1), bleaching (Sect. 3.2), framework (Sect. 3.6) |
| (S) ArEw | $n = 24$ n/a | Easton Wood, UK | 52°21.43′ N | 1°41.52′ E | Early Pleistocene (2.35–2.25 Ma) | Biostratigraphic evidence | Mayhew (2013) | Framework (Sect. 3.6) |
| (T) ArAh | $n = 6$ n/a | Alderton House Pit TM330415, UK | 52°1.2′ N | 1°23.24′ E | Late Pliocene, Early Pleistocene (3.6–2.12 Ma) | Lithological, biostratigraphic evidence | BGS (2024), Hamblin et al. (1997) | Framework (Sect. 3.6) |
| (U) ArCg | $n = 3$ n/a | Capel Green Pit TM376496, UK | 52°4.41′ N | 1°27.5′ E | Late Pliocene, Early Pleistocene (3.6–2.12 Ma) | Lithological, biostratigraphic evidence | BGS (2024), Hamblin et al. (1997) | Framework (Sect. 3.6) |
| Range finding (multiple names; see Table S2) | $n = 73$ | Fladen Ground (North Sea) | Various[c] | Various[c] | Unknown | None | n/a | Range finding (Sect. 3.7) |
| Range finding (multiple names; see Table S2) | $n = 87$ | North Icelandic shelf | Various[c] | Various[c] | Unknown | None | n/a | Range finding (Sect. 3.7) |

[a] Note: beach-collected samples could range thousands of years in age (e.g. Dominguez et al., 2016). [b] Further detail on radiocarbon dates are in Table S1 in the Supplement. [c] Further information about sampling location is in Table S2. n/a: not applicable

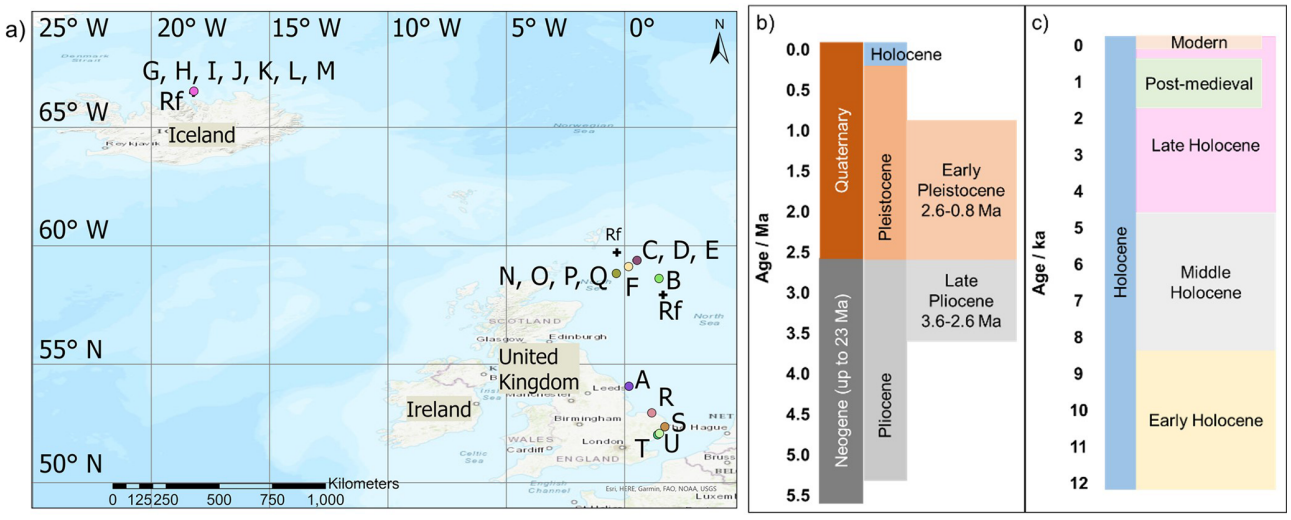


**Figure 2.** **(a)** Location of the *A. islandica* samples analysed in this work. Map created using ArcGIS Pro. Geological timeline of the **(b)** Pliocene, Pleistocene, and Holocene on a 1-million-year scale and of the **(c)** Holocene on a 1000-year scale (IUGS International Chronostratigraphic Chart, 2023).

ventral margin of the shell, likely containing a few annual growth increments. To build the AAG framework (Sect. 3.7), intact Quaternary shells were subsampled near the margin of the shell where the iOSL was thickest. Fragmented shells were sampled where the iOSL was thickest for ease of sampling. Between each sample the drill tip was cleaned in a 0.6 M HCl (Fisher, analytical grade) solution and MeOH (Fisher, HPLC grade) to reduce cross-contamination of samples.

### 2.3 Bleaching procedure

Following protocols developed by Penkman et al. (2008), approximately 20–30 mg of powder was transferred to a 2 mL plastic microcentrifuge tube (Eppendorf), and NaOCl (12 %, VWR, 50 µL $mg^{-1}$ of sample) was added. Samples were oxidized for 24–72 h for bleaching experiments (Sect. 3.3). Following the results of these experiments, the iOSL layer of all other subfossil samples was oxidized for 48 h. After the allotted time, the NaOCl was removed, and the powder was washed six times with deionized water (18.2 MΩ $cm^{-1}$) and once with MeOH (Fisher, HPLC grade). The samples were left to air-dry for 1–2 d.

### 2.4 High-temperature experiments

High-temperature experiments were carried out in a BINDER ED 23 oven set to 140 °C. To the bleached powder (10–20 mg), 300 µL of deionized water (18.2 MΩ $cm^{-1}$) was added in a glass vial (Penkman et al., 2008). The samples were exposed to high-temperature conditions of 140 °C for 8, 24, and 48 h. After this time, the water was carefully removed, and the powder was left to air-dry for 1–2 d.

### 2.5 Isolation of free amino acids (FAAs) and total hydrolysable amino acids (THAAs)

Following bleaching and in some cases high-temperature exposure, the dry powder (1–10 mg) was split between free amino acids (FAAs) and total hydrolysable amino acids (THAAs; Penkman et al., 2008). The FAAs were demineralized in 2 M HCl (10 µL $mg^{-1}$ of sample, minimum possible volume) and dried over a rotary vacuum concentrator (Christ RVC 2-25 CDplus, 1300 rpm). The THAA samples were hydrolyzed in 7 M HCl (20 µL $mg^{-1}$ of sample) and heated at 110 °C for 24 h to hydrolyse the peptide bonds. The samples were then dried in a rotary vacuum concentrator.

### 2.6 UHPLC-FLD analysis

Samples were rehydrated with a solution containing an internal standard – L-homo-arginine (0.01 mM), sodium azide (1.5 mM), and HCl (0.01 M) – to enable quantification of the amino acids. Analysis of chiral amino acid pairs was achieved using an Agilent 1200 Series HPLC fitted with an Agilent Eclipse Plus C18 column (4.6 × 100 mm, 1.8 µm particle size) and fluorescence detector (excitation wavelength 230 nm, emission wavelength 445 nm) using a UHPLC method modified from Crisp (2013; Table 2). The binary mobile phase consisted of (A) sodium acetate buffer (23 mM sodium acetate trihydrate, sodium azide, and 1.3 µM EDTA, adjusted to pH 6.00 ± 0.01 with 10 % acetic acid and sodium hydroxide) and (B) 92.5 : 7.5 methanol : acetonitrile. Table 2 reports the mobile phase, flow rate, and temperature gradient of the separation. Data processing was performed on ChemStation, and data analysis was performed in Excel; all data discussed in this paper are reported in Table S2 in the

Supplement. The Crisp (2013) method is able to separate the L and D enantiomers of 14 amino acids.

### 2.7 Powder XRD analysis

Powder X-ray diffraction analysis was carried out on a selection of samples (Table 1) using a Malvern Panalytical Aeris powder XRD scanned between 0–70° $2\theta$ using a 0.2° increment per second. The scan axis was Gonio, the source filter was beta nickel, the beam mask was set to 20, the beam knife was set to high, and anti-scatter was 9 mm. The samples analysed were powdered either by a rotary burr on a drill (Sect. 2.2) or by homogenizing to a fine powder with an agate pestle and mortar. Homogenized *Cepaea* spp. shells were used as aragonite standards, and modern ostrich eggshell (OES) was used as the calcite standard.

## 3 Results and discussion

The multilayer nature of *A. islandica* (comprising the oOSL, iOSL, and ISL; Fig. 1) means that there are likely to be protein differences between layers. This will dictate the original amino acid concentration and composition, and therefore their diagenesis, with impacts on D/L values and AAG. Initially we present an assessment of the mineralogy (Sect. 3.1), followed by the results from bleaching (Sect. 3.2) and heating experiments on the three microstructural layers (Sect. 3.3), assessing the amino acid composition, concentration, and D/L values. Ontogenetic trends on modern and subfossil shells are presented in Sect. 3.4. Recommendations for the method for AAG analysis of *A. islandica* (Sect. 3.5) are followed by an initial AAG framework over the Quaternary period (Sect. 3.6) and application of the method to age range-finding undated shells (Sect. 3.7).

### 3.1 Assessment of sampling procedure and mineral diagenesis

Aragonite, the polymorph of $CaCO_3$ that makes up the three layers of the shells of *A. islandica*, can convert into calcite over geological timescales or under stress (Brand and Morrison, 1987). The transition state in the transformation of labile aragonite into calcite can have implications for the integrity of any closed system and the IcP (Preece and Penkman, 2005; Penkman, 2010). Thus, investigating the mineral composition of samples may help to identify compromised samples; this can be done using X-ray diffraction. In order to understand any potential changes to the $CaCO_3$ structure, powder XRD was carried out on a selection of samples of a variety of ages to qualitatively assess the presence of aragonite and/or calcite (Table 1).

The diffractograms of modern (shells A and F), post-medieval (shell H), mid-Holocene (shell Q; Walker et al., 2019), and Early Pleistocene (shell R) shells that were drilled show a small peak of calcite ($\theta$ 29°) in the mainly aragonitic shells (Fig. 3a). There is no clear pattern between the age of the sample and the presence or absence of calcite; the Early Pleistocene shell (shell R, 2.2–2.1 Ma) shows only a very small calcite peak compared to larger peaks in the modern and post-medieval shells. Individual burial conditions will impact the potential for mineral diagenesis in a sample, but it is also possible that the abrasion and temperature created during the drilling process may affect the aragonitic crystal structure (Baldreki et al., 2024). To test this, drilled powders were compared with shell chips from the same samples homogenized with a pestle and mortar (Fig. 3b). The chips do not show a calcite peak at $2\theta$ 29° (Fig. 3b); these experiments indicate that any diagenetic calcite was below the limits of detection for these samples and that the drilling process caused some transformation of aragonite into calcite. However the drilling process is necessary in order to remove the periostracum and to isolate and sample the required layers for AAG in this shell type. Other methods to remove the periostracum include using a scalpel and dipping the shell in HCl, NaOH, or $H_2O_2$ (Checa, 2000; Agbaje et al., 2018), but it is challenging to isolate the individual mineralized layers without drilling. Therefore, it is important to use the lowest speed possible and avoid applying extreme pressure when sampling using a rotary drill.

### 3.2 The impact of bleaching on amino acids

To test for any presence of an intra-crystalline protein fraction, bleaching experiments on each of the layers of *A. islandica* in three shells (Table 1) was undertaken: two modern samples (shell A, beach-collected, and shell B, trawled) and an Early Pleistocene sample (shell R).

In the modern samples, the concentration of FAAs and THAAs in all layers decreases with bleaching (Fig. 4), meaning that an inter-crystalline fraction is removed. There is an initial sharp decrease and a subsequent very small increase in concentration after 24 h in the oOSL layer of shell B, possibly indicating that the prolonged bleaching process is breaking some of the peptide bonds, increasing the concentration of amino acids from the intra-crystalline fraction. In the iOSL and ISL layers of shells A and B, the concentration reaches a plateau (i.e. little or no change in trend between two or more observations) between 48 and 72 h, indicating that an intra-crystalline fraction is more resistant to bleaching than the unbleached shells and therefore requires long oxidation exposure. This isolated intra-crystalline fraction represents $17 \pm 3$ % (all errors represent $1\sigma$ around the mean) of the oOSL, $16 \pm 5$ % of the iOSL, and $15 \pm 2$ % of the ISL in the unbleached FAA fraction of shell B. The total concentration in the FAA fraction is 1.5–2 orders of magnitude smaller than in the THAA fraction; as the sample is young there would have been little natural breakage of the peptide bonds to form free amino acids. Following an initial drop in concentration from 0–24 h, the concentration is stable in the THAA fraction with increasing bleaching time in all layers in both shells.

**Table 2.** Gradient of mobile phase, flow rate, and column temperature for the UHPLC-FLD method. * indicates that the parameter does not change at the referred time point.

| Time (min) | % A sodium acetate buffer | % B 92.5 : 7.5 methanol : acetonitrile | Flow rate (mL min$^{-1}$) | Column temperature (°C) |
|---|---|---|---|---|
| 0.0 | 90 | 10.0 | 1.25 | 25 |
| 8.8 | 82.0 | 18.0 | 1.25 | * |
| 10 | 82.0 | 18.0 | 1.25 | 28 |
| 11 | 82.0 | 18.0 | 1.25 | 28 |
| 23 | 78.3 | 21.7 | 1.25 | 28 |
| 25 | 78.3 | 21.7 | 1.25 | 28 |
| 32 | 75.2 | 24.8 | 1.25 | 28 |
| 34.5 | 74.0 | 26.0 | 1.25 | 28 |
| 36 | 65.0 | 35.0 | 1.25 | 28 |
| 50 | * | * | 1.30 | 25 |
| 56 | 50.0 | 50.0 | 1.30 | 25 |
| 62 | 2.0 | 98.0 | 1.30 | 25 |
| 67 | 95.0 | 5.0 | 1.25 | 25 |

This intra-crystalline fraction represents $13 \pm 0.5$ % of the oOSL ($\sigma = 1$), $10 \pm 1$ % of the iOSL ($\sigma = 1$), and $15 \pm 1.5$ % of the ISL in the total unbleached THAA fraction for shell A. For shell B the bleached amino acids represent $7 \pm 0.1$ % of the oOSL and the iOSL ($\sigma = 1$) and $18 \pm 1$ % of the ISL. In summary, the FAAs and THAAs in the intra-crystalline fraction are stable and isolated between 24–48 h of bleaching in the modern *A. islandica* shell.

The geological formation of free amino acids through peptide bond hydrolysis is evident in the Early Pleistocene shell from Weybourne Crag (shell R; Fig. 5). Similarly to the modern sample, the Early Pleistocene FAAs and THAAs decrease in concentration with bleaching; the variability between replicates is larger so identification of the plateau is more challenging, potentially lying between 48 and 72 h in both the THAA and FAA fractions. Sykes et al. (1995) noted that solid slices of modern *A. islandica* were less susceptible to 10 % NaOCl oxidation compared to the shell powder – in the latter, aspartic acid concentration reached a plateau after 10 h – indicating that the intra-crystalline fraction for the powdered shell was isolated after just 10 h of oxidation. In our study, when the individual shell layers are isolated and powdered, a concentration plateau is only achieved between 24 and 48 h (Fig. 5); in contrast to the results from Sykes et al. (1995), we therefore suggest that bleaching for 48 h is necessary to securely isolate the intra-crystalline protein fraction. In the Early Pleistocene shell, the percentage of intra-crystalline fraction compared to the unbleached FAA fraction is $61 \pm 5$ % in the oOSL, $38 \pm 5$ % in the iOSL, and $70 \pm 7$ % in the ISL; for the THAA fraction the intra-crystalline fraction represents $49 \pm 5$ % of the oOSL, $30 \pm 1$ % of the iOSL, and $55 \pm 6$ % of the ISL. Due to the age of the shell, it is not surprising that the majority of the FAAs are intra-crystalline, with the more labile inter-crystalline free amino acids likely to have leached out of the system (Sykes et al., 1995). Despite the age of the shell ($\sim$ 2.2–2.1 Ma), there are both inter- and intra-crystalline amino acids present (Demarchi, 2009; Penkman et al., 2007; Demarchi et al., 2013a, b; Ortiz et al., 2015, 2018). It is interesting to note that the ISL and oOSL layers contain a higher relative percentage of intra-crystalline protein (oOSL $= 49 \pm 5$ % and ISL $= 55 \pm 6$ %), whereas the iOSL has a much lower proportion of IcP ($30 \pm 1$ %).

As the oxidation step has been shown to induce some racemization in other mollusc shells, especially with long exposure (Penkman et al., 2008), when choosing the optimal bleaching time both concentration and racemization have to be considered. In the modern and Early Pleistocene samples there is an initial increase in D/L for Asx (aspartic acid), Glx (glutamic acid), Ser (serine), Ala (alanine), and Val (valine) between 0–24 h bleaching, indicating that the removal of the inter-crystalline protein leaves more racemized amino acids in the IcP (Penkman et al., 2008). The D/L values reach a plateau between 24 and 48 h, and at the 72 h time point the D/L values slightly increase for most amino acids, suggesting that some oxidation-induced racemization is taking place (Fig. 6). Nevertheless, the concentration plateau reached at 48 h in both the modern and Early Pleistocene samples and the small change in D/L values indicate that the intra-crystalline protein fraction is effectively stable and relatively protected from oxidation.

The percentage composition of each amino acid in the bleached and unbleached samples can provide information about the nature of protein in the two fractions, if different. The composition of the unbleached shell and IcP is similar for the THAA fraction, but some differences are present in the FAA fraction in the modern sample (Figs. 7, S1). In this fraction, in the bleached samples of shell B, Gly (glycine) is much higher, and Ser, Ala, and Arg (arginine) are lower; however, this may be due to the very low concentrations of minor amino acids, sometimes below the limit of detection.

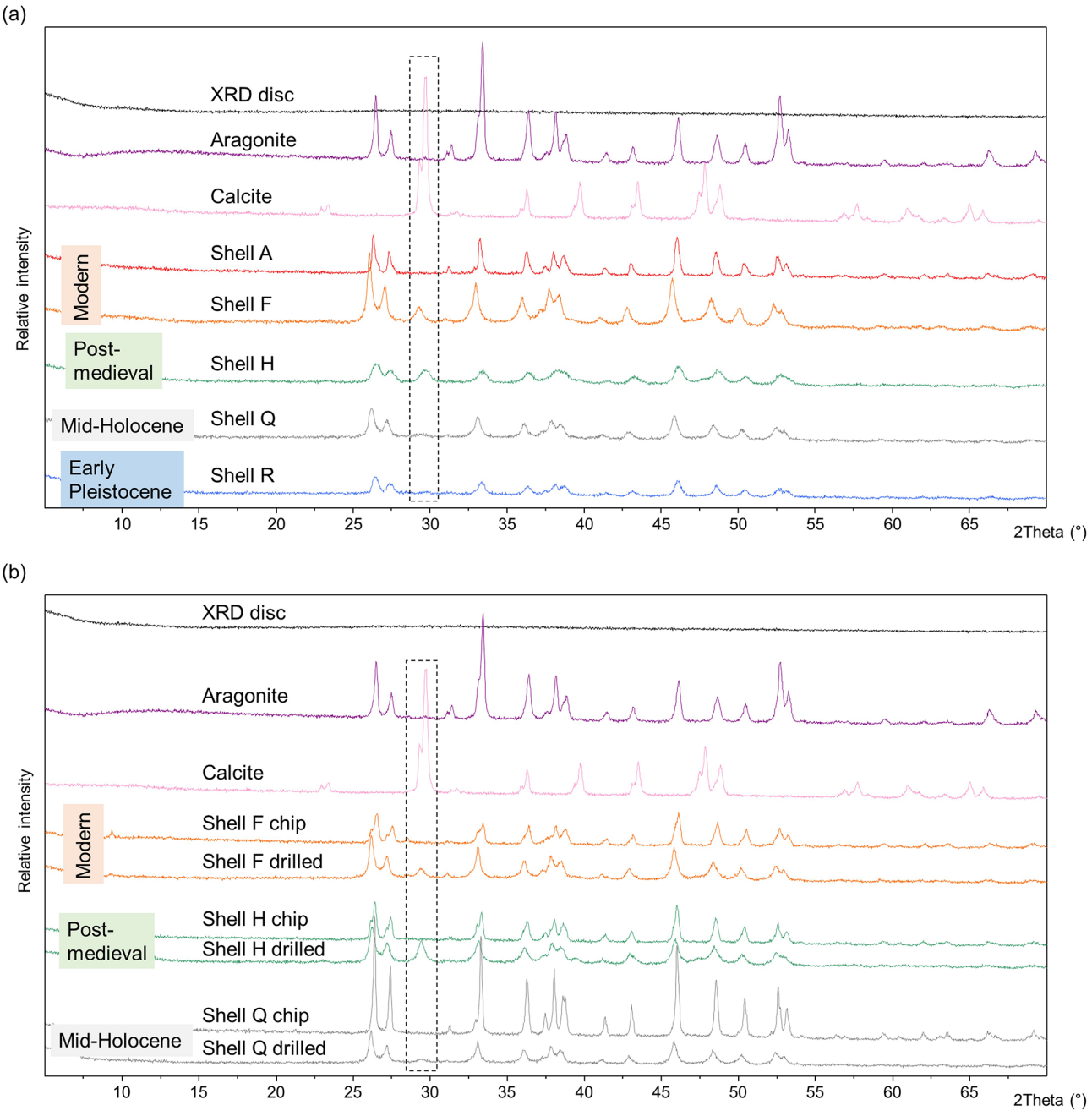


**Figure 3.** **(a)** pXRD spectra of *A. islandica* shells of various ages, powdered using a drill. **(b)** pXRD spectra of *A. islandica* shells. In each case the same shell was drilled with a rotary burr ("drilled") and homogenized with a pestle and mortar ("chip"). The areas within the dashed black lines represent the main peak of calcite at $2\theta$ 29°. As the drilling process may convert aragonite into calcite, it must be undertaken with care.

In the Early Pleistocene sample, the composition is very similar between the unbleached and bleached fractions in both the FAAs and THAAs (Fig. S2), confirming that the majority of amino acids in the unbleached samples are intracrystalline and that much of the inter-crystalline protein fraction has leached out with time.

In addition to differences in amino acid concentration between the three layers of *A. islandica*, there are also slight differences in composition between layers. In the THAA fraction of the modern shells bleached for 48 h, all three layers have similar composition, with some exceptions: Ala is higher in the iOSL and Arg is lower in the ISL than in the other two layers for shell B. Shell A shows slightly lower

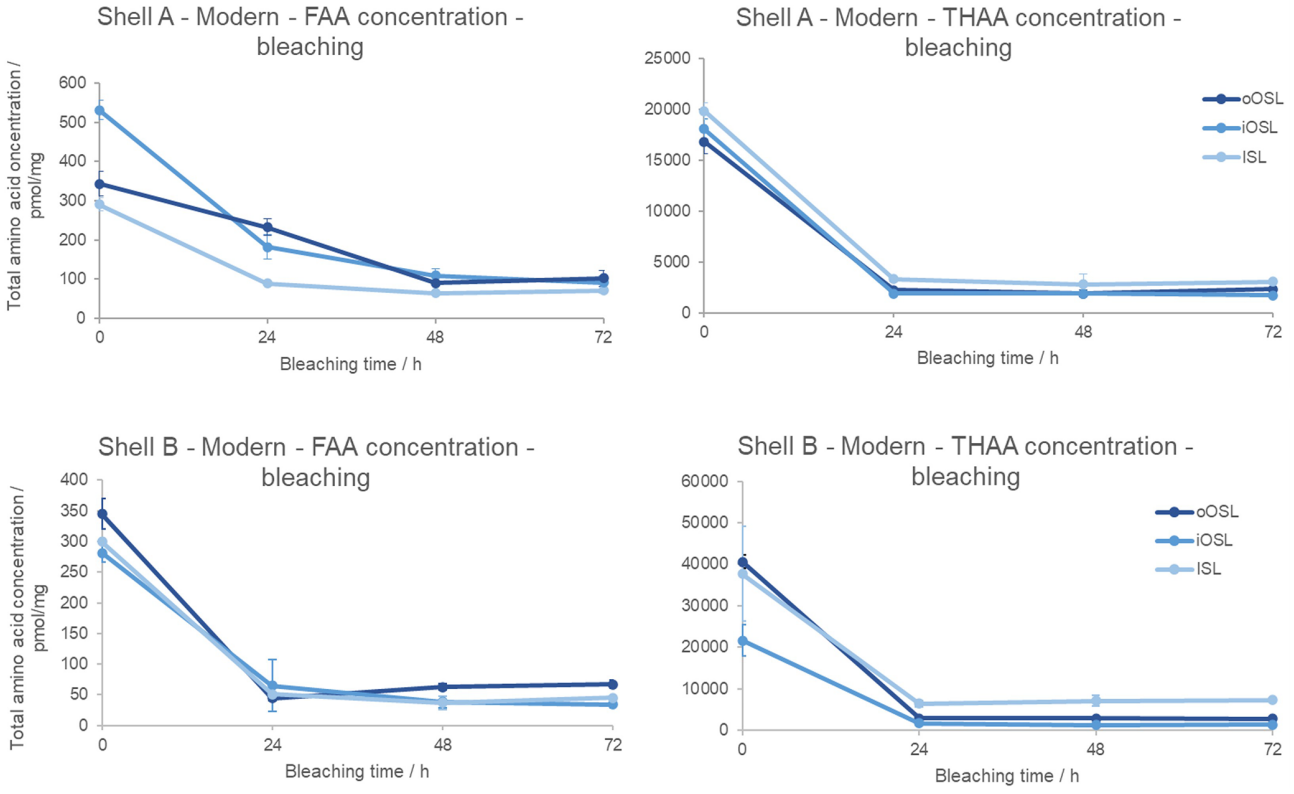


**Figure 4.** Decrease in total amino acid concentration upon bleaching modern *Arctica islandica* (shell A from Bridlington Beach, UK, and B from the North Sea off Peterhead, UK) for the oOSL, iOSL, and ISL microstructural layers. Error bars indicate 1 standard deviation about the mean based on two replicates (shell A) and three replicates (shell B). Note the large drop in concentration with bleaching, with a plateau reached by 48 h.

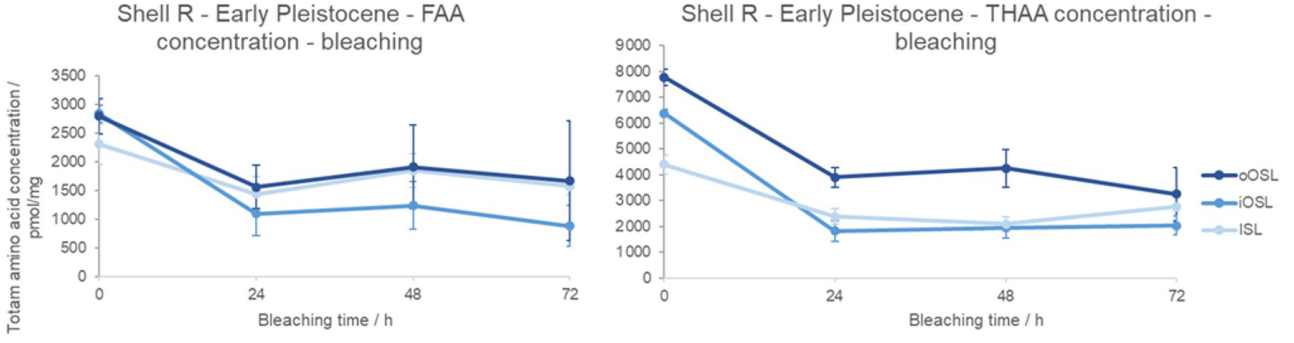


**Figure 5.** Change in total amino acid concentration upon bleaching Early Pleistocene *A. islandica* (shell R from Weybourne Crag, UK) for the oOSL, iOSL, and ISL microstructural layers. Error bars indicate 1 standard deviation about the mean based on two replicates. Note the drop in concentration with bleaching, with a plateau reached by 48 h within error bars.

composition of Asx and Glx in the oOSL compared to the other two layers and also to shell B; however, the variability between samples is larger for these amino acids in shell A than in shell B, complicating interpretation. The percentage composition of Gly is slightly higher in the oOSL than in the iOSL and ISL for both shells A and B, although the between-sample variability is larger than for the other two layers, which may confound the results for shell B (Fig. 7). In the Early Pleistocene shell, the FAA fraction shows very similar composition between the three layers. In the THAA fraction, the ISL and iOSL contain higher amounts of Asx and Glx, while Thr (threonine) is more abundant in the two OSL layers and Gly is highest in the ISL layer. There is mostly agreement in the composition of the two shells. The higher

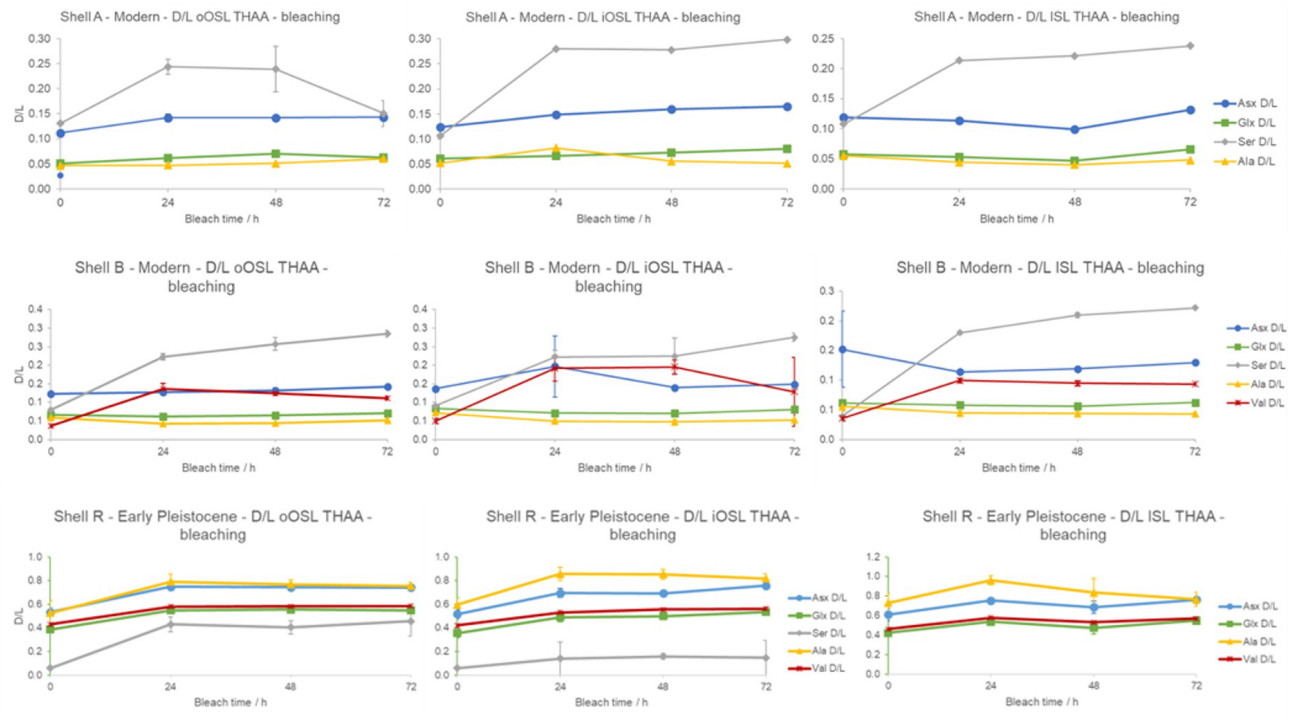


**Figure 6.** Mean THAA D/L of Asx, Glx, Ser, Ala, and Val in *A. islandica* upon bleaching for the oOSL, iOSL, and ISL microstructural layers. Top row: modern shell from Bridlington Beach (shell A); error bars indicate 1 standard deviation based on three replicates. Middle row: modern shell from the North Sea (shell B); error bars indicate 1 standard deviation based on three replicates. Bottom row: Early Pleistocene shell from Weybourne Crag (shell R); error bars indicate 1 standard deviation based on two replicates. There is an initial increase in D/L with bleaching but stable D/L with prolonged bleaching.

percentage composition of Gly in the Early Pleistocene shell is likely to be due to the natural diagenesis of Val (valine), Ser, Thr, and Tyr (tyrosine) to form Gly (Vallentyne, 1964). Ser is much lower and Ala is higher in the Early Pleistocene samples: Ser is thermally unstable and can degrade to form Ala and Gly (Vallentyne, 1964; Bada et al., 1978), while Ala can be a product of dehydration of Ser and Asx (Walton, 1998). The overall differences in amino acid composition in both modern and Early Pleistocene shells for the three layers shows that originally there are different proteins in the layers, which then break down at different rates; therefore, it is important to consistently sample one layer for reliable AAG.

Haugen and Sejrup (1990) presented the percentage composition of 30 modern unbleached specimens of *A. islandica* for both the inner and outer shell layers; as there was no separation into oOSL and iOSL, their results for the "outer" layer are compared to our oOSL and iOSL results (Fig. S1b). Additionally, Haugen and Sejrup (1990) analysed their amino acid with ion-exchange chromatography rather than HPLC, and they do not report His (histidine), Arg, and Met (methionine). The percentage composition of the FAA and THAA fractions from the modern shell B analysed here and the 30 shells from Haugen and Sejrup (1990) are very similar, with only small variations (Fig. S1b). In the FAA fraction there is a lower contribution from Tyr in our data (3 %–4 %) compared to 13 %–15 % in the Haugen and Sejrup (1990) shells, while Gly is higher in our data for the bleached shells (44 %–67 %) but more comparable in the unbleached samples (31 %–34 % for our work and 21 %–24 % for that of Haugen and Sejrup, 1990). In the THAA fraction the percentage compositions from Haugen and Sejrup (1990) are within error with our bleached data, while our unbleached shell has higher Gly and lower Asx and Glx. There is a remarkable similarity in percentage composition between Haugen and Sejrup (1990) results without bleaching and our modern bleached shells; this may ultimately enable the comparison between data from samples analysed prior to and after establishing the bleaching step in the AAG method.

A recent study compared the percentage composition of amino acids in untreated and oxidized modern shells, including 12 % NaOCl treatment on powdered shell where the layers had been homogenized (Huang et al., 2023). Similar to our results, Gly, Asx, and Glx were the dominant amino acids in the unbleached shells, followed by Ala, Ser, and Thr (Fig. S1a). Upon bleaching, Pro (proline) was the most abundant amino acid (Huang et al., 2023), but this secondary amino acid is not quantified in the current analytical method used for AAG. As in our bleaching experiments, in the work of Huang et al. (2023), upon bleaching Gly decreased in composition, while Asx, Glx, Ala, Val, Arg, and Phe showed an

increase in composition; other amino acids present in lower concentrations show no trend or an opposite trend. There is therefore a general agreement between the study from Huang et al. (2023) and our current work, with the differences possibly due to the sampling approach: Huang et al. (2023) homogenized all three aragonitic layers after removing the periostracum, whereas our study separates the oOSL, iOSL, and ISL, providing a more detailed study of the amino acid composition in the three microstructural layers.

### 3.3 Elevated temperature experiments to test for closed-system behaviour

High-temperature experiments are considered a controlled, simple way to assess the suitability of biomineral proteins for AAG (Kriausakul and Mitterer, 1978; Haugen and Sejrup, 1992; Penkman et al., 2008; Hendy et al., 2012; Demarchi et al., 2013b). The resistance of the IcP to oxidation was shown with bleaching experiments on modern and Pleistocene shells (Sect. 3.2). To test whether the IcP behaves like a closed system, the bleached powder (48 h) from the three layers of modern *A. islandica* shell B (Table 1) was exposed to high temperatures in hydrous conditions (140 °C for 8, 24, and 48 h), and the protein degradation (including rates of racemization) was observed. The high-temperature experiments are utilized to accelerate the protein degradation and explore the processes that would otherwise occur over thousands of years. Previous studies showed that the degradation patterns in high-temperature heating experiments do not necessarily produce the same degradation patterns in subfossil samples; low-temperature treatment ($\sim$ 80 °C) may be more similar to subfossil results but requires long exposure (Crisp et al., 2013; Tomiak et al., 2013; Demarchi et al., 2013b). Nevertheless, the chosen temperature of 140 °C allows a quick assessment of protein degradation patterns and leaching over a short timescale (a few days), while trends in concentration and D/L values and correlations of FAA and THAA D/L with increased exposure to 140 °C can provide evidence on whether the amino acids in *A. islandica* behave as a closed system (Penkman et al., 2008).

The total concentration of FAAs in the intra-crystalline fraction increases over time because prolonged heating breaks the peptide bonds to ultimately release free amino acids (Fig. 8). The total THAA concentration decreases with heating due to the decomposition of amino acids (Penkman et al., 2008; Crisp et al., 2013; Tomiak et al., 2013; Demarchi et al., 2013b), discussed in detail below. An interesting observation is that the ISL layer has a higher THAA concentration than the other layers but also has a steep increase in FAA concentration with heating time, coinciding with a steep drop in THAA concentration. This means that the amino acids in the inner layer (ISL) are more susceptible to peptide bond hydrolysis, and in the hydrolysable fraction (which includes both bound and free AAs) they are more prone to decomposition than in the outer layer. This may be due to differences in the proteins' primary sequence or higher structures or to a result of the way the proteins are mineral-bound in the ISL microstructure. Conversely, the concentration of FAAs and THAAs in the iOSL layer shows the least change, indicating that the protein in this layer may be more resistant to degradation.

The different rates of breakdown of the three layers indicate the importance of consistently sampling one microstructure for obtaining more reliable AAG results.

If *A. islandica* resembles a closed system the diagenetic products of protein degradation would be retained; thus the FAA and THAA D/L would be highly correlated (Preece and Penkman, 2005; Penkman et al., 2007; Demarchi et al., 2011, 2015). As expected, the D/L values for all amino acids increase with increased heating duration in all layers (Figs. 9a, S3), meaning that racemization patterns follow reliable trends in the intra-crystalline protein fraction in *A. islandica*. Figure 9b shows the correlation of FAA and THAA for Asx, Glx, Ser, Ala, Tyr, Val, and Phe: overall, all amino acids from all layers show high co-variance indicative of closed-system behaviour. However, some scattering is observed for the ISL layer. There is also some scattering for Ser, especially in the outer layers, which is expected in these high-temperature experiments (Bright and Kaufman, 2011; Crisp et al., 2013) because the thermally unstable Ser (the "parent") readily degrades into Gly and Ala (the "products"). It is expected that the ratio of the "parent" over a degraded product will decrease with heating and thus indicate increased decomposition (Bada et al., 1978). This is particularly evident after 8 h heating with a marked reduction in the ratio of [Ser] / [Ala] (Fig. 10). In the THAA fraction Ser D/L decreases after 24 h (Fig. S4) due to decomposition of free serine, resulting in a decrease in the overall racemization of Ser (Penkman, 2010).

Other decomposition pathways include the degradation of Ser, Thr, and Tyr (the "parent") into Gly (Vallentyne, 1964) and of Asx (the "parent") into Ala (Walton, 1998). These trends were observed in all cases in the FAA and THAA samples of the iOSL layer after 8 h and in the oOSL layer after 24 h, whereas in the ISL layer the ratios increased in some cases (Fig. S4). As previously mentioned for the concentration and D/L values, this could either be due to how the different peptides are bound to the mineral or to differences in protein sequence and structure in the ISL layer compared to the outer layers. Upon heating, the concentration of FAA increases at a high rate in the ISL (Fig. 8), and the steep "parent"-product ratios may reflect the more labile nature of the peptide bonds. The THAA composition of the bleached unheated ISL layer also shows a higher percentage of the more labile "parent" amino acids Asx, Thr, and Tyr compared to the outer layers, while Ser has similar composition in all three layers (Fig. S5). Therefore, the high proportion of amino acids with labile peptide bonds in the ISL explains the high decomposition rate of FAAs (Fig. 8) and the faster degradation rates.

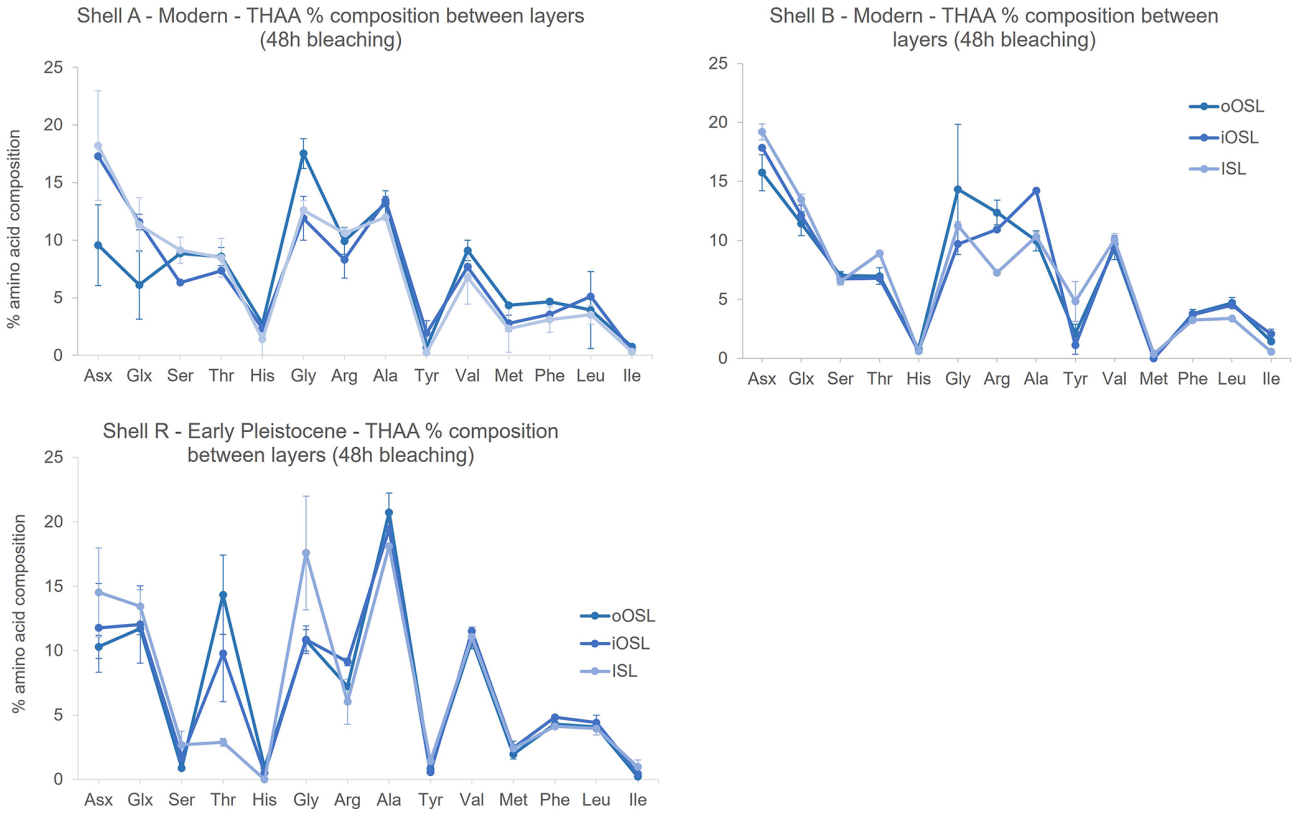


**Figure 7.** Mean THAA percentage composition after 48 h of bleaching in the three microstructural layers of *A. islandica* from modern samples (shell A from Bridlington and shell B from the North Sea) and from an Early Pleistocene sample (shell R). Error bars represent 1 standard deviation based on three replicates for shell B and two replicates for shells A and R. There are differences in amino acid composition between the three aragonitic layers in the modern and Early Pleistocene shells, indicating differences in original protein composition.

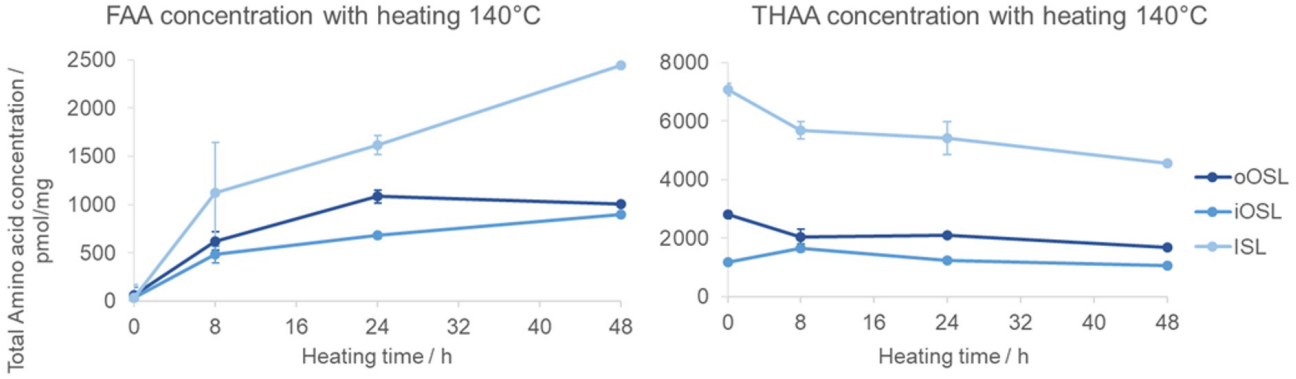


**Figure 8.** FAA and THAA concentration changes with heating at 140 °C in the three shell layers of modern *A. islandica* shell B. Error bars indicate 1 standard deviation based on three replicates. The FAA concentration increases with heating due to peptide bond hydrolysis; the ISL seems to have faster peptide bond hydrolysis compared to the other layers.

The high correlation between FAA and THAA D/L values and the predictable degradation pattern observed from the high-temperature experiments point towards a closed-system behaviour for *A. islandica* in all three layers However, these differences in rates of degradation between the inner and outer layers would affect the D/L values and the accuracy of the AAG interpretation; therefore it is preferable to analyse one specific layer. Interestingly, in the ISL a high proportion of amino acid is lost to hydrolysis in the THAA fraction and to degradation in the FAA fraction. In isotope studies the oOSL is not used because it can be more readily contaminated or impacted by environmental factors,

it being the most external layer (Schöne, 2013). The iOSL is routinely used in isotope analyses and can be used in sclerochronology (Schöne and Huang, 2021; Butler et al., 2009). Due to the previous research on the iOSL, our bleaching and high-temperature degradation experiments, and ease of sampling the iOSL, we therefore suggest using this same layer for AAG.

### 3.4 Assessing ontogenetic trends in modern and subfossil AAG

Previous work on amino acid $\delta^{15}$N of *A. islandica* has shown changes in isotope values and amino acid composition with ontogeny, i.e. with the biological age of the shell (Schöne and Huang, 2021). Here, the iOSL of eight shells with a known lifetime spanning 100–400 years (Table 1) were sampled near the hinge (representing the early ontogenetic age of the shell) and near the margin (representing late ontogeny) to check for any differences in composition and D/L values. Given the importance of original protein composition to the subsequent degradation, it is important to determine whether there are differences in concentration and D/L between early and late ontogeny as seen in amino acid isotopic analyses (Schöne and Huang, 2021). In addition, if the rates of the reactions are fast enough, it may be possible to use AAG for age resolution *within* an individual shell. For example, AAG has been used in sclerochronological studies of tropical *Porites* corals (e.g. Goodfriend et al., 1992), providing a resolution of ±6 years in most recent material and ±24 years in the last 150 years (Hendy et al., 2012). In these cases the ability to obtain high-resolution data was due to the relatively high ambient temperatures (∼ 26 °C; Hendy et al., 2012) in which the corals live, but the lower temperatures of *A. islandica*'s habitat (∼ 1–16 °C; Schöne, 2013) mean that AAG for sclerochronology may not be applicable to this biomineral.

It is expected that the iOSL of samples from early ontogeny will have higher D/L values because this part of the biomineral would have been deposited earlier in time; late ontogenetic samples will have lower D/L values. As the fastest-racemizing amino acids (Figs. 9a, S3), Asx, Ser, and Ala were examined in detail (Fig. 11). The error bars are quite large in the FAA samples, likely due to the low concentrations of amino acids, so the data should be treated with caution; therefore only the THAAs are going to be discussed here. In the mid-Holocene samples the D/L values for Asx, Ser, and Ala show higher values in late ontogeny, contrary to the expectation (Fig. 11a). The intra-shell variability is very low ($\sigma = 0.005$–$0.02$ for FAAs and THAAs), and the lack of ontogenetic trend is likely related to the older age of the shells confounding the in vivo degradation. The post-medieval shells do not show any significant ontogenetic pattern (Fig. 11b). The expected higher D/L values in early ontogeny are present in the modern shells in FAA Asx, THAA Asx, and Ser D/L plots but not for Ala (Fig. 11c). Similarly to our data, Goodfriend and Weidman (2001) showed a gradual decrease in D/L in the unbleached outer layer of modern *A. islandica* shells from the umbo to the rim, but the trend was less evident in subfossil shells, especially in increments older than $1050 \pm 35$ ($^{14}$C age). The increments in early ontogeny also showed a much higher extent of racemization connected with fast growth and large band ages compared to the rest of the shell, indicating that there are different proteins responsible for shell growth in early and late ontogeny (Goodfriend and Weidman, 2001). As a result, they recommended consistent sampling of the iOSL layer in late ontogeny or at least after increment year 20 (Goodfriend and Weidman, 2001).

It is notable that the D/L values in the THAA fraction of modern samples in early ontogeny follow the year of birth in the THAA fraction (Fig. 11c), meaning that the oldest shell that first settled from larva in 1865 has the highest D/L (Fig. 11b; shell C, blue circle), followed by the shell represented by the orange circle (Fig. 11b; shell D) which settled in 1874, and the least racemized sample is the shell that settled in 1908 (Fig. 11b; shell E, grey circle). For the post-medieval shells, intra-shell variation is high, especially for the D/L values corresponding to ∼ 1400 CE. Similarly, the late ontogeny modern shells (Fig. 11c; shell C, D, E) all died in 2004 and should have similar D/L values, but they show great variability and/or large error bars, except for the FAA Asx D/L values.

The concentration of amino acids is higher in early ontogeny samples in the mid-Holocene shells from the North Sea, whereas the opposite trend is observed in the post-medieval and modern shells (Fig. S6). Goodfriend and Weidman (2001) observed a slight decrease in the percentage composition of Ser, Tyr, Met, Ile, and Leu with age and an increase in that of Glu, Val, Ala, and Asp with age. Overall, there is no specific trend in composition with ontogeny in our shells, although some of the palaeontological and modern shells show similar results to Goodfriend and Weidman (2001), indicating that there may be more acidic intracrystalline proteins responsible for growth during early ontogeny compared to late ontogeny, where basic amino acids are more prominent (Fig. S6). The different proteins in early and late ontogeny may also be responsible for the variability in D/L. In summary, the D/L values in early and late ontogeny of the modern, post-medieval, and mid-Holocene ages have high intra-shell and inter-shell variability, suggesting that AAG is not suitable for providing chronologies within *A. islandica* shells. Given the possible variability in D/L values and protein composition with ontogeny, it is recommended to consistently sample the iOSL layer for AAG; late ontogeny is preferred because of the increased thickness of the iOSL layer.

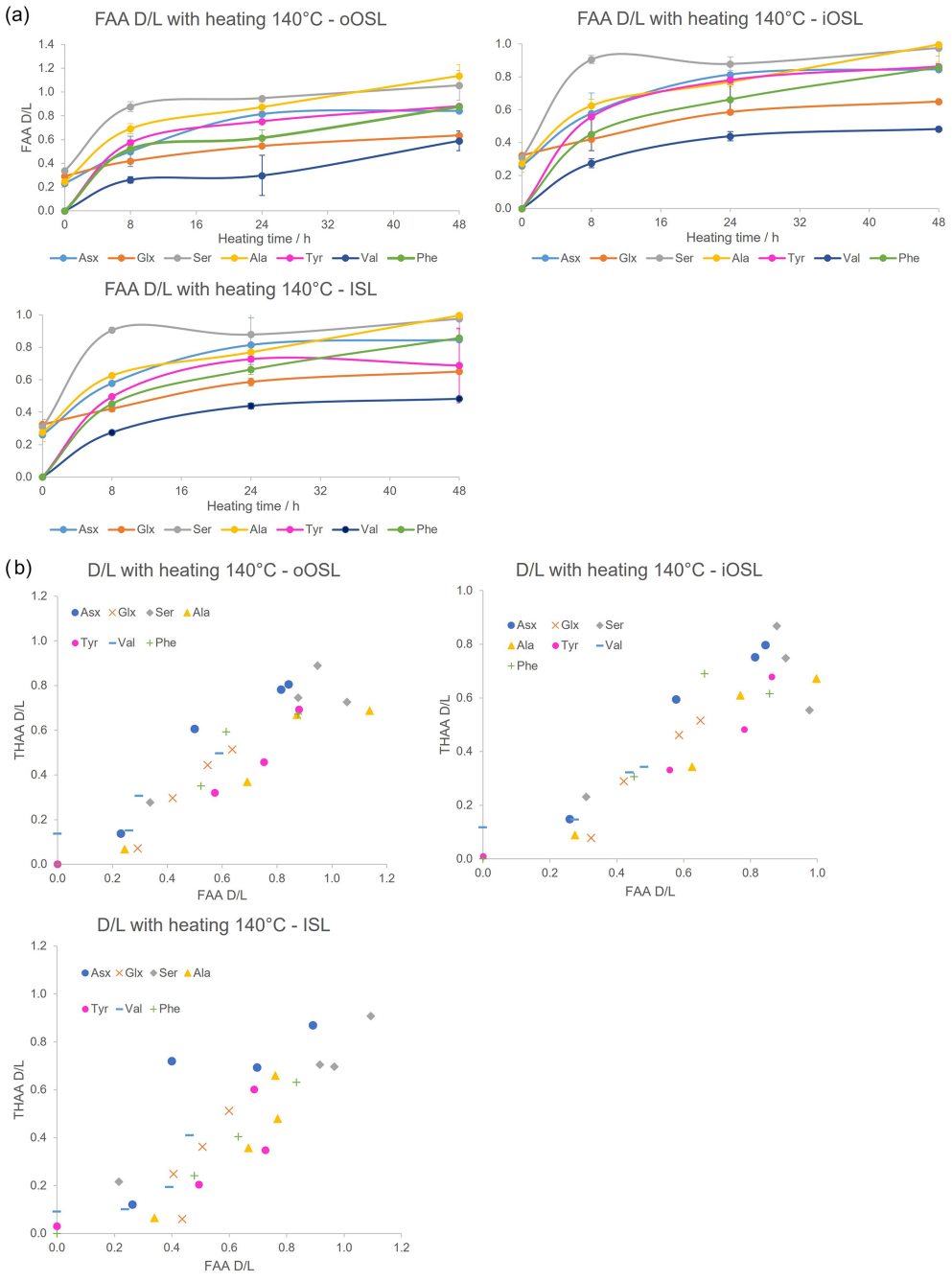


**Figure 9.** **(a)** Mean FAA D/L with increased duration of heating at 140 °C in the three bleached layers of modern *A. islandica* (shell B); error bars indicate 1 standard deviation based on three replicates. **(b)** FAA vs. THAA D/L with heating at 140 °C. D/L values increase with increasing exposure to high temperature in all three aragonitic layers and high correlation between the FAA and THAA fractions in most cases.

### 3.5 Optimized method and recommendations

The bleaching experiments have shown that the IcP of all three microstructural layers can be isolated after 48 h of bleaching (Figs. 4–5; Sect. 3.2). Heating experiments showed that all layers behave as a closed system. The ISL has a higher rate of peptide bond hydrolysis (Fig. 8), likely due to the higher percentage composition of labile amino acids compared to the outer layers. The slightly higher scattering in D/L values in the ISL (Fig. 9b) suggests the use of the outer shell layer for future dating. The low peptide bond hydrolysis and co-variance between FAAs and THAAs in the oOSL and iOSL suggests that these layers may provide more reliable dating (Sect. 3.3). Given that the iOSL is easier for sampling,

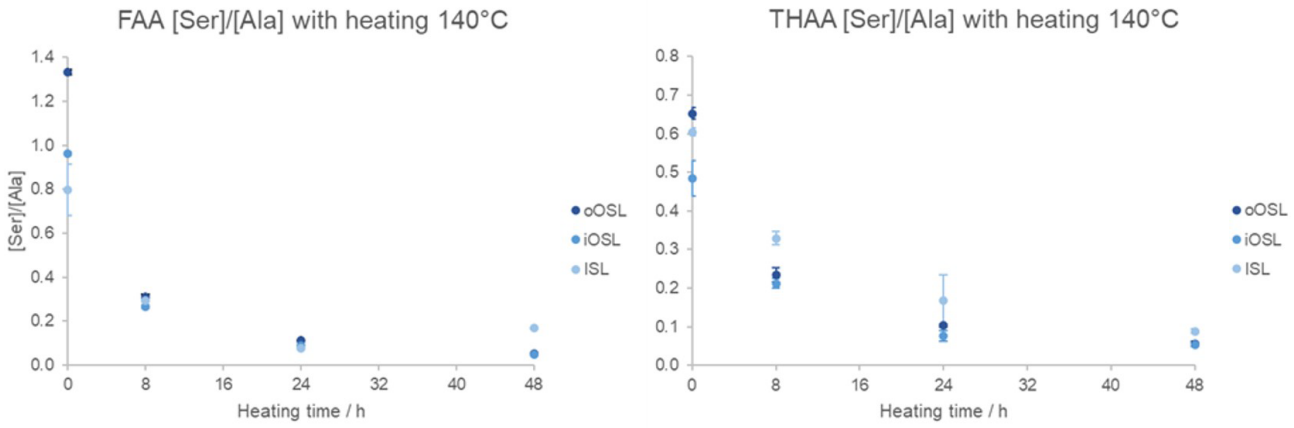


**Figure 10.** [Ser] / [Ala] in the bleached oOSL, iOSL, and ISL layers of modern *A. islandica* (shell B) following heating at 140 °C for 8–48 h. Error bars indicate 1 standard deviation based on three replicates. The [Ser] / [Ala] decreases with heating in all three aragonitic layers.

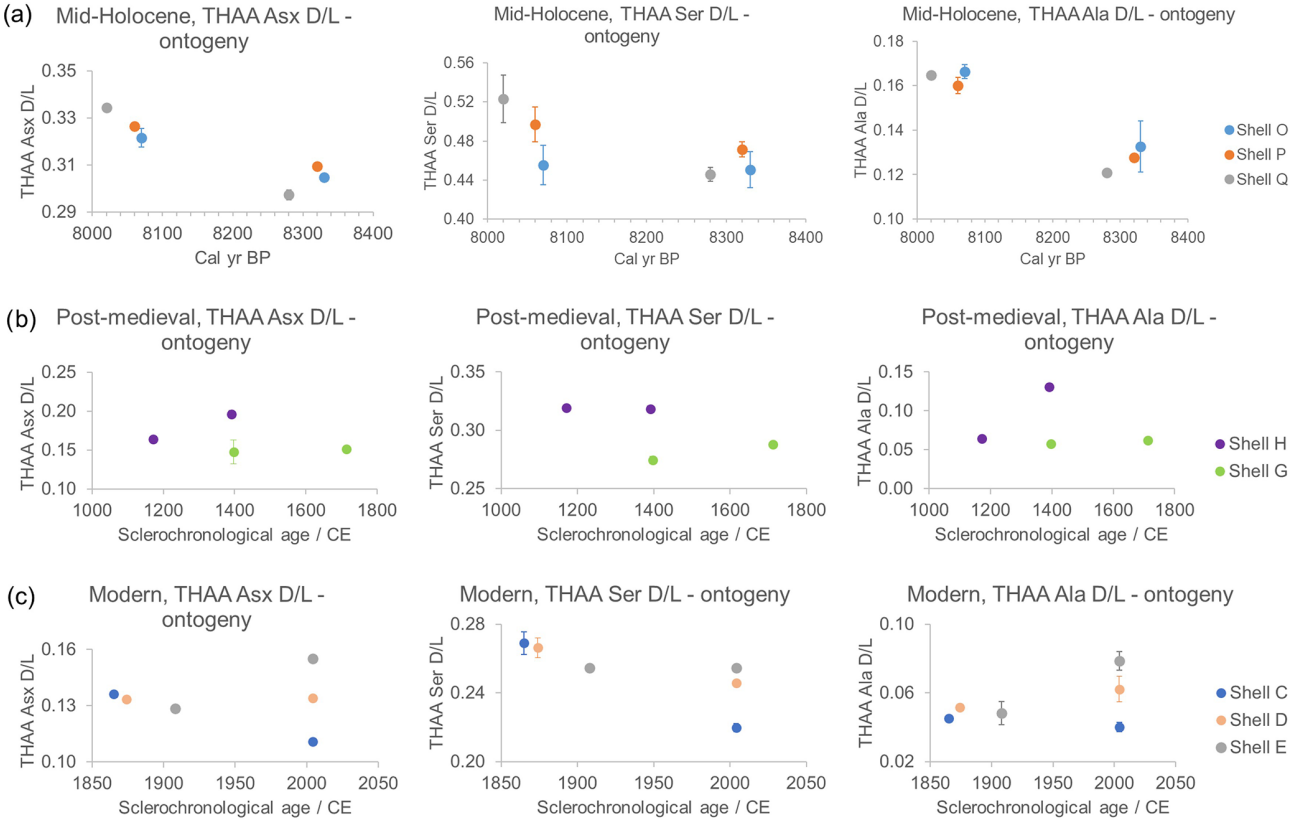


**Figure 11.** THAA Asx, Ser, and Ala D/L for **(a)** mid-Holocene (shells O, P, Q), **(b)** post-medieval (shells G, H), and **(c)** modern *A. islandica* (shells C, D, E) early- and late ontogeny samples. Note that the ages of mid-Holocene samples were assigned with radiocarbon dating, while for post-medieval and modern shells the age is based on sclerochronological cross-dating. The age sampled for AAG may vary slightly from the sclerochronological age reported. Error bars indicate 1 standard deviation based on two analytical replicates. Except for the modern samples, AAG shows no ontogenetic trends.

as this layer is the widest and is already used in sclerochronological and isotope studies, we recommend using this layer for AAG. From the ontogenetic trends observed (Sect. 3.4), it is recommended to sample the late ontogeny (near the margin) portion of the iOSL; this should ensure more consistent protein analysis.

In conclusion, for AAG analysis of *A. islandica* we recommend cleaning of the shell in deionized water with sonication

and selective drilling of the iOSL from a portion deposited in late ontogeny. The drilling step can be done by slicing the shell from the umbo to the margin (Sect. 2.2) and then either selectively drilling the iOSL with a handheld rotary burr if this layer is thick or drilling the oOSL away until the iOSL is reached and collecting only the latter layer. Caution needs to be taken to continuously move the rotary burr to reduce the build-up of temperature that can degrade the protein (Sect. 3.1). The powdered iOSL is then exposed to NaOCl for 48 h and removed by washing with water and MeOH. The demineralization, hydrolysis, and UHPLC analysis steps are outlined in Sect. 2.

### 3.6 An initial IcPD AAG framework for *A. islandica*

Following the isolation of a stable intra-crystalline protein fraction that shows effectively closed-system behaviour in the iOSL of *A. islandica* in laboratory experiments, we analysed subfossil shells with independent evidence of age to observe the degradation patterns of amino acids in *A. islandica* during the Quaternary and late Pliocene periods. The subfossil shell samples used in this initial framework were *A. islandica* already established by sclerochronological cross-dating, radiocarbon dating, subfossil evidence, lithology, biostratigraphy, and AAG of other material in the same horizon (Table 1; Butler et al., 2009, 2013; Estrella-Martinez, 2019; Preece et al., 2020; Hamblin et al., 1997; Table S2). The iOSL was sampled, when possible, from late ontogeny for consistency of results. Samples were prepared as outlined in Sects. 2 and 3.5.

In a closed system the FAA and THAA D/L values are highly correlated and indicate that both fractions of amino acids degrade predictably. From the high-temperature experiments (Sect. 3.3) Asx and Ser were the fastest racemizers, meaning that they should provide higher temporal resolution for dating more recent specimens. Glx, Val, and Phe show slower racemization (Fig. S3); thus they may be able to separate Early Pleistocene and late Pliocene shells and to date earlier in the Pliocene period. In our subfossil samples the FAA and THAA D/L show a high co-variance for Asx and good correlation of THAA Glx, Ser, and Asx (Fig. 12), indicating that subfossil samples follow a predictable degradation pattern.

In some amino acid parameters there seem to be different degradation patterns when comparing the high-temperature experiments and subfossils (Fig. S7). This has been seen before in other biominerals (e.g. Tomiak et al., 2013; Dickinson et al., 2019; Baldreki et al., 2024) and may be due either to limitations of these high-temperature experiments or to different degradation pathways which are enabled under high-temperature conditions. Both preclude using this high-temperature dataset to calculate kinetic parameters for this biomineral. The 24 shells from Easton Wood (shell S) show tight clustering of D/L values for 19 shells, while 4 specimens have lower D/L Asx and Val and 1 specimen has higher FAA Val and Ala D/L values than the cluster (Fig. S8). In addition, these shells also have a different percentage composition of amino acids (Asx, Glx, Phe, and Ala), indicating that the closed-system behaviour of these 5 shells may have been compromised (Preece and Penkman, 2005; Penkman et al., 2007; Penkman and Wenban-Smith, 2013; Demarchi et al., 2015). Therefore, we removed these 5 specimens from the framework (Fig. 12). Nevertheless, these tests have shown that D/L values and amino acid composition are useful tools to identify outliers, providing a more accurate framework for future analyses.

While the IcP framework is richer in the Holocene period and very limited for the Pleistocene, the late Pliocene, Early Pleistocene, and mid-Holocene samples are well-separated for the amino acids presented here, showing that it is possible to distinguish between Pleistocene and Holocene samples using *A. islandica* (Fig. 12). However, using Glx and Val (Fig. 12a, c, d), it is not possible to distinguish between the modern and post-medieval shells. In the Asx and Ser plot (Fig. 12b) the modern, post-medieval, and late Holocene (Walker et al., 2019) shells are better separated, although some overlap is still present. In this plot, the THAA Ser values for the late Pliocene and Early Pleistocene shells are undetected or lower than in modern shells because free Ser naturally decomposes with age, as previously shown in the heating experiments (Sect. 3.3) and in other biominerals (Penkman et al., 2008; Penkman, 2010; Crisp et al., 2013; Kaufman et al., 2013; Demarchi et al., 2013b, 2015; Ryan et al., 2020).

These preliminary results indicate that it is possible to use the IcP in the iOSL of *A. islandica* for AAG of Quaternary shells. The late Pliocene and Early Pleistocene shells have very high D/Ls for the fast racemizer Asx (FAA Asx D/L $\sim$ 0.85–0.99; THAA Asx D/L $\sim$ 0.69–0.90), approaching the end point for using Asx in AAG (Torres et al., 2013; Demarchi et al., 2011). Glx and Val D/L values were lower (FAA Glx D/L $\sim$ 0.62–0.75, Val D/L $\sim$ 0.75–0.95; THAA Glx D/L $\sim$ 0.50–0.66, Val D/L $\sim$ 0.56–0.88), meaning that there is potential to use these slower racemizers to date shells further back into the Pleistocene and late Pliocene (Fig. 12c, d; Penkman et al., 2007; Reichert et al., 2011; Hendy et al., 2012; Torres et al., 2013; Demarchi et al., 2013b; Millman et al., 2022). On the Holocene timescale, the fast racemizers Asx and Ser provide reliable D/L separation between the middle and late Holocene (Fig. 12f). Modern samples have a slight overlap with post-medieval shells in THAA Ser and Asx, meaning that the resolution of AAG for *A. islandica* for these amino acids may be approx. 1500–2000 years during the middle and late Holocene in the temperate-cold climate of the North Sea. Given the non-linear nature of AAG, the resolution will be reduced into the Pleistocene, but further analyses are required to assess the resolution. If samples date from the last $\sim$ 50 ka, then radiocarbon dating will provide a higher-resolution dating method compared to AAG in the temperate-cold environment where *A. islandica* typically

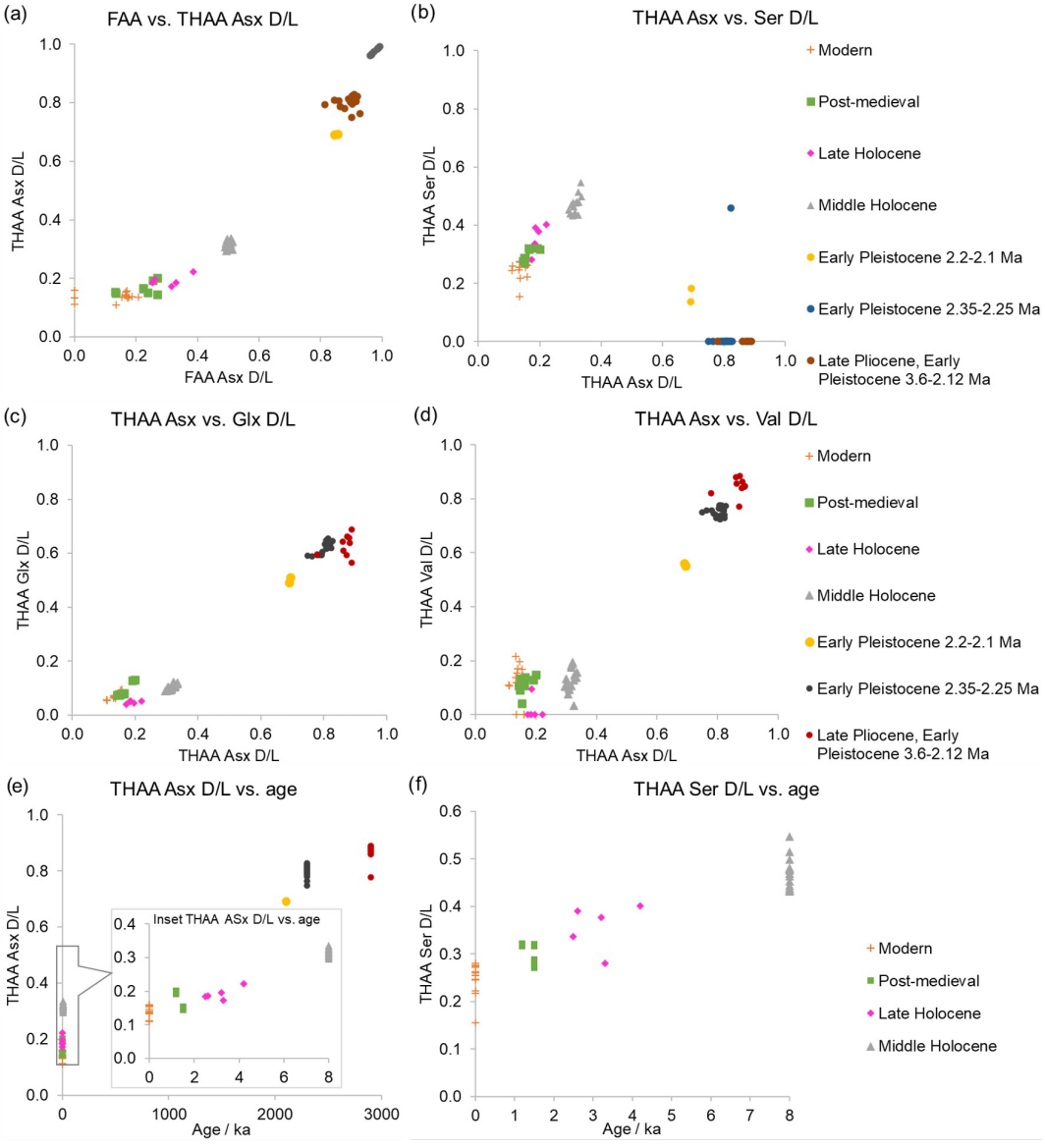


**Figure 12.** **(a)** FAA vs. THAA Asx D/L; **(b)** THAA Asx vs. Ser D/L; **(c)** THAA Asx vs. Glx D/L; **(d)** THAA Asx vs. Val D/L; **(e)** THAA Asx D/L vs. age and inset focusing on the last 8 ka; and **(f)** THAA Ser D/L vs. age of modern, post-medieval, late Holocene, middle Holocene, Early Pleistocene and late Pliocene *A. islandica* shells. D/L values for the slower-racemizing amino acids (e.g. Glx and Val) span the Quaternary period, while the faster-racemizing amino acids (e.g. Asx and Ser) allow temporal resolution within the Holocene.

lives, although it requires correction for the marine reservoir effect (Hajdas et al., 2021). Nevertheless, AAG using the IcP of the iOSL of *A. islandica* has the potential to discriminate middle and late Holocene samples and further back into the Early Pleistocene and late Pliocene.

### 3.7 AAG range finding of undated shells

Since the middle and late Holocene, important cultural transitions and palaeoenvironmental and ecological changes, both natural and human-induced, have taken place in the North Sea and Iceland and had an impact on the marine ecosystem (for example, the Mesolithic–Neolithic transition, the settlements of Vikings in Iceland, and the Industrial Revolution in northern Europe (Andersen, 2000; Ahronson, 2012; Poulsen, 2008). The palaeoenvironmental record contained within subfossil *A. islandica* provides a unique way to study these important transitions, but dating is required to identify potentially relevant shells. As part of the ERC SEACHANGE project, over 20 000 *A. islandica* shells were collected from the North Sea and Iceland seafloors during research cruise DY150 in 2022, with the aim to use these for geochemical and sclerochronological studies (Scourse et al., 2022). Here we explore the potential for range-finding age

estimates of individual dead shells by AAG. The initial IcPD AAG framework showed the potential to provide dating of shells with a resolution of 1500–2000 years during the middle and late Holocene. The range finding is expected to narrow down the age of the shells collected from the North Sea and Iceland seafloors (Table S2).

The AAG age range finding was carried out on the iOSL laid down during late ontogeny of 160 shells (Fig. 13; Table S2). The AAG dating determined that these shells likely span the middle and late Holocene, with both the Asx and Ser D/L values in agreement with this time period. In cases where there was agreement between the three most useful parameters for the Holocene (FAA Asx D/L, THAA Asx D/L, and THAA Ser D/L), the narrowest age range possible was assigned (Fig. 13). It is noted that there are a few shells that overlap between age periods, likely due to the resolution of AAG. In cases where there was agreement between two of the three D/L values, a wider age range was assigned. For example, shell Ic22200193 showed correlation with the late Holocene for the THAA Asx and Ser D/Ls, but the FAA Asx D/L value overlapped between the late Holocene and post-medieval age; due to the agreement of two of the three parameters with the late Holocene (which includes post-medieval), this shell was assigned an age range correlating with this stage. Shell FG22202523 showed THAA Asx D/L, indicating a modern age, but FAA Asx D/L and THAA Ser D/L overlap between the modern and post-medieval ages, thus a post-medieval–modern age range was assigned. These three screening methods resulted in 93 shells with a narrower age range and 67 shells with a wider age range (either due to agreement of two of the three D/Ls or overlap of D/L values between age ranges). There were four shells, Ic22201300, Ic2220035, Ic22200194, and Ic22202048, which showed D/L values consistently higher than the late Holocene shells but lower than the mid-Holocene shells; thus, they were categorized as older than ∼ 4 ka and younger than ∼ 8 ka in age (8 ka < shells > 4 ka). A total of 10 shells from the Fladen Ground exhibited THAA Asx and Ser D/L values slightly higher than the mid-Holocene D/L values; thus they were categorized as early Holocene or older. The results of AAG range finding of *A. islandica* show that this technique is able to narrow down the ages of shells, assigning 10 shells to the early Holocene or older, 7 shells as younger than ∼ 8 ka and older than ∼ 4 ka (8 ka < shells > 4 ka), 23 shells to the late Holocene, 34 shells to the post-medieval age, and 86 shells to the modern age. These analyses provide an initial age range for *A. islandica* shells which, depending on the time period of interest, can then enable the selection of appropriate shells for more accurate radiocarbon dating and consequently better-constrained sclerochronological cross-dating.

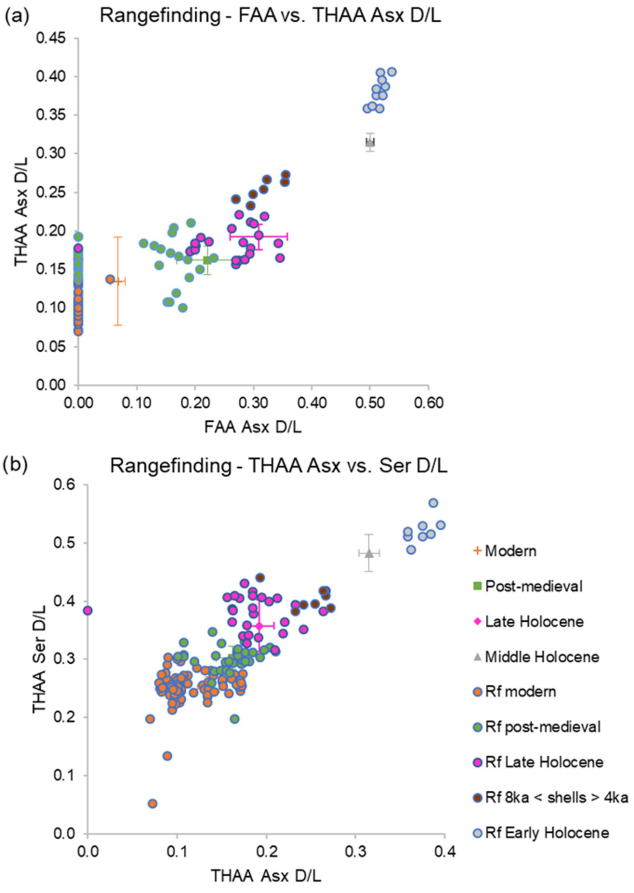


**Figure 13.** Range finding (Rf) of *A. islandica* shells within the IcPD framework: **(a)** FAA vs. THAA Asx D/L and **(b)** THAA Asx vs. Ser D/L. Modern samples are in orange, post-medieval in green, late Holocene shells in pink, shells older than ∼ 4 ka and younger than ∼ 8 ka (8 ka < shells > 4 ka) in brown, and early Holocene in grey.

## 4 Conclusion

A protocol for the analysis of intra-crystalline chiral amino acids for amino acid geochronology (AAG) of the bivalve *A. islandica* has been established. The three-layer microstructure of the shell has been investigated to determine which layer would be most applicable to AAG. The intracrystalline protein (IcP) fraction was successfully isolated with NaOCl oxidation for 48 h. This analysis highlighted different amino acid compositions between the three layers (oOSL, iOSL, and ISL), meaning that for reliable dating a single microstructural layer should be sampled. Heating experiments at 140 °C showed that the protein fraction in the inner layer (ISL) is more prone to peptide bond hydrolysis than the outer layers, possibly due to the high composition of labile amino acids in this layer. Conversely, the outer layers show low loss and decomposition of amino acids. Nevertheless, all three layers show good co-variance between FAA and THAA D/L and behave as a closed system. The iOSL layer is recommended for AAG because it

is already used for isotopic and sclerochronological studies. The oOSL, the outermost layer, is more exposed to the external environment and marine organisms and is thinner than the iOSL, thus harder to sample. Samples of early and late ontogeny in modern, post-medieval, and mid-Holocene shells did not show a consistent pattern of composition and D/L; thus the resolution and sensitivity of AAG is too low for sclerochronological studies *within A. islandica* shells of this age. The optimized method of analysis of the iOSL, following bleaching for 48 h, was applied to Quaternary and late Pliocene subfossils, providing an initial dating framework, with the fast racemizers Asx and Ser able to distinguish mid-Holocene from post-medieval and/or modern samples, providing a tentative resolution for AAG of *A. islandica* of approx. 1500 years in the late Holocene. The slower-racemizing amino acids are able to date back to at least the late Pliocene, and Val and Glx can separate Pliocene from Early Pleistocene specimens. Range finding of 160 undated shells showed that AAG can securely separate between modern, post-medieval ($\sim$ 1100–1700 CE), late Holocene (4–1 ka), mid-Holocene ($\sim$ 8 ka), and early Holocene ($>$ 8 ka) shells. Further analyses are required to expand the framework and better establish the age resolution for this biomineral, but these initial promising results indicate that the intracrystalline fraction of the iOSL in *A. islandica* is a reliable biomineral for AAG dating of marine deposits during the Quaternary and late Pliocene periods and therefore for range-finding collections of *A. islandica* shells of unknown age.

**Data availability.** Data in this study have been included in Table S2, and all amino acid data from this study will be made available through the NOAA repository upon publication: https://www.ncei.noaa.gov/pub/data/paleo/aar/ (last access: 9 May 2024; NOAA, 2024).

**Supplement.** The supplement related to this article is available online at: https://doi.org/10.5194/gchron-6-175-2024-supplement.

**Author contributions.** Conceptualization: KEHP and JDS. Data curation: MLGC. Formal analysis: MLGC and KEHP. Funding acquisition: KEHP, JDS. Investigation: MLGC and KEHP. Methodology: MLGC and KEHP. Project administration and supervision: KEHP and JDS. Resources: KEHP, MLGC, PGB, DJR, TT, and JDS. Validation: MLGC, PGB, DJR, TT, JDS, and KEHP. Visualization: MLGC and KEHP. Writing (original draft preparation): MLGC and KEHP. Writing (review and editing): MLGC, KEHP, PGB, DJR, TT, and JDS.

**Competing interests.** At least one of the (co-)authors is a member of the editorial board of *Geochronology*. The peer-review process was guided by an independent editor, and the authors also have no other competing interests to declare.

**Disclaimer.** Publisher's note: Copernicus Publications remains neutral with regard to jurisdictional claims made in the text, published maps, institutional affiliations, or any other geographical representation in this paper. While Copernicus Publications makes every effort to include appropriate place names, the final responsibility lies with the authors.

**Acknowledgements.** Collection of the Easton Wood shells was funded by the European Research Council (ERC) under the European Union's Horizon 2020 research and innovation programme (grant no. 865222). We thank Dustin White, Richard Preece, Tim Holt-Wilson, and Matthew Jeffries for collecting the shells from Easton Wood.

We thank Jake Scolding, Anna Genelt-Yanovskaya, and Elizabeth Harper for providing some of the samples, as well as Niklas Hausmann for discussing initial sampling techniques and for providing samples. Sam Presslee and Matt von Tersch are thanked for initial laboratory training and Sheila Taylor for administrative support. Adrian Whitwood is thanked for initial training on powder X-ray diffraction. We are grateful to Lucy Wheeler, Marc Dickinson, and Chloë Baldreki for helpful comments on an initial version of this paper.

**Financial support.** The SEACHANGE Synergy Project has received funding from the European Research Council (ERC) under the European Union's Horizon 2020 research and innovation programme (grant no. 856488).

Iceland radiocarbon dates were funded by the EU Framework 6 MILLENNIUM Integrated Project "European climate of the last millennium" (SUSTDEV-2004-3.1.4.1, 017008-2).

North Sea radiocarbon dates were funded by the European Union Fifth Framework HOLSMEER project (EVK2-CT-2000-00060) and the United Kingdom Natural Environment Research Council standard research grant (NER/A/S/2002/00809).

**Review statement.** This paper was edited by Irka Hajdas and reviewed by two anonymous referees.

## References

Abelson, P. H.: Organic constituents of fossils, Carnegie Inst. Wash. YRB, 54, 97–101, 1955.

Agbaje, O. B. A., Shir, I. B., Zax, D. B., Schidt, A., and Jacob, D. E.: Biomacromolecules within bivalve shells: Is chitin abundant?, Acta Biomater., 80, 176–187, https://doi.org/10.1016/j.actbio.2018.09.009, 2018.

Ahronson, K.: Seljaland: archaeology, palaeoecology and tephrochronology, in: Holocene Tephrochronology. Applications in South Iceland. Field Guide, edited by: Larsen, G. and Eiríksson, J., Quaternary Research Association, London, 61–66, 2012.

Alves, E. Q., Macario, K., Ascough, P., and Bronk Ramsey, C.: The worldwide marine radiocarbon reservoir effect: Definitions, mechanisms, and prospects, Rev. Geophys., 56, 278–305, https://doi.org/10.1002/2017RG000588, 2018.

Andersen, S. H.: "Køkkenmøddinger" (shell middens) in Denmark: A survey, P. Prehist. Soc., 66, 361–84, 2000.

Bada, J. L., Shou, M. Y., Man, E. H., and Schroeder, R. A.: Decomposition of hydroxy amino acids in foraminiferal tests; kinetics, mechanism and geochronological implications, Earth Planet. Sc. Lett., 41, 67–76, https://doi.org/10.1016/0012-821X(78)90042-0, 1978.

Baldreki, C., Burnham, A., Conti, M., Wheeler, L., Simms, M. J., Barham, L., White, T. S., and Penkman, K.: Investigating the potential of African land snail shells (Gastropoda: Achatininae) for amino acid geochronology, Quat. Geochronol., 79, 101473, https://doi.org/10.1016/j.quageo.2023.101473, 2024.

Baleka, S., Herridge, V. L., Catalano, G., Lister, A. M., Dickinson, M. R., di Patti, C., Barlow, A., Penkman, K. E. H., Hofreiter, M., and Paijmans, J. L. A.: Estimating the dwarfing rate of an extinct Sicilian elephant, Curr. Biol., 31, 3606–3612.e7, https://doi.org/10.1016/j.cub.2021.05.037, 2021.

Brand, U. and Morrison, J. O.: Paleoscene #6. Biogeochemistry of fossil marine invertebrates, Geosci. Can., 14, 85–107, 1987.

Bridgland, D. R., Harding, P., Allen, P., Candy, I., Cherry, C., George, W., Horne, D. J., Keen, D. H., Penkman, K. E. H., Preece, R. C., Rhodes, E. J., Scaife, R., Schreve, D. C., Schwenninger, J.-L., Slipper, I., Ward, G. R., White, M. J., White, T. S., and Whittaker, J. E.: An enhanced record of MIS 9 environments, geochronology and geoarchaeology: data from construction of the High Speed 1 (London–Channel Tunnel) rail-link and other recent investigations at Purfleet, Essex, UK, Proc. Geol. Assoc., 124, 417–476, https://doi.org/10.1016/j.pgeola.2012.03.006, 2013.

Bright, J. and Kaufman, D. S.: Amino acids in lacustrine ostracodes, part III: Effects of pH and taxonomy on racemization and leaching, Quat. Geochronol., 6, 574–597, https://doi.org/10.1016/j.quageo.2011.08.002, 2011.

BGS – British Geological Survey, Red Crag Formation, https://data.bgs.ac.uk/id/Lexicon/NamedRockUnit/RCG, last access: 16 February 2024.

Brooks, A. S., Hare, P. E., Kokis, J. E., Miller, G. H., Ernst, R. D., and Wendorf, F.: Dating Pleistocene archeological sites by protein diagenesis in ostrich eggshell, Science, 248, 60–64, 1990.

Brosset, C., Höche, N., Shirai, K., Nishida, K., Mertz-Kraus, R., and Schöne, B. R.: Strong coupling between biomineral morphology and Sr/Ca of Arctica islandica (Bivalvia) – Implications for shell Sr/Ca-based temperature estimates, Minerals, 12, 500, https://doi.org/10.3390/min12050500, 2022.

Butler, P. G., Richardson, C. A., Scourse, J. D., Witbaard, R., Schöne, B. R., Fraser, N. M., Wanamaker, A. D., Bryant, C. L., Harris, I., and Robertson, I.: Accurate increment identification and the spatial extent of the common signal in five Arctica islandica chronologies from the Fladen Ground, northern North Sea, Paleoceanography, 24, PA2210, https://doi.org/10.1029/2008PA001715, 2009.

Butler, P. G., Wanamaker, A. D., Scourse, J. D., Richardson, C. A., and Reynolds, D. J.: Variability of marine climate on the North Icelandic Shelf in a 1357-year proxy archive based on growth increments in the bivalve Arctica islandica, Palaeogeogr. Palaeocl., 373, 141–151, https://doi.org/10.1016/j.palaeo.2012.01.016, 2013.

Checa, A.: A new model for periostracum and shell formation in Unionidae (Bivalvia, Mollusca), Tissue Cell, 32, 405–406, https://doi.org/10.1054/tice.2000.0129, 2000.

Crippa, G., Azzarone, M., Bottini, C., Crespi, S., Felletti, F., Marini, M., Petrizzo, M. R., Scarponi, D., Raffi, S., and Raineri, G.: Bio- and lithostratigraphy of lower Pleistocene marine successions in western Emilia (Italy) and their implications for the first occurrence of Arctica islandica in the Mediterranean Sea, Quaternary Res., 92, 549–569, https://doi.org/10.1017/qua.2019.20, 2019.

Crisp, M. K.: Amino acid racemization dating: Method development using African ostrich (Struthio camelus) eggshell, PhD thesis, University of York, 2013.

Crisp, M., Demarchi, B., Collins, M., Morgan-Williams, M., Pilgrim, E., and Penkman, K.: Isolation of the intra-crystalline proteins and kinetic studies in Struthio camelus (ostrich) eggshell for amino acid geochronology, Quat. Geochronol., 16, 110–128, https://doi.org/10.1016/j.quageo.2012.09.002, 2013.

Davies, B. J., Bridgland, D. R., Roberts, D. H., Cofaigh, C. Ó., Pawley, S. M., Candy, I., Demarchi, B.: The age and stratigraphic context of the Easington Raised Beach, County Durham, UK, Proc. Geol. Assoc., 120, 183–198, 2009.

Demarchi, B.: Geochronology of coastal prehistoric environments: a new closed system approach using amino acid racemisation, PhD thesis, University of York, 2009.

Demarchi, B., Williams, M. G., Milner N., Russell, N., Bailey, G., and Penkman, K.: Amino acid racemization dating of marine shells: A mound of possibilities, Quaternary Int., 239, 114–124, https://doi.org/10.1016/j.quaint.2010.05.029, 2011.

Demarchi, B., Collins, M. J., Tomiak, P. J., Davies, B. J., and Penkman, K. E. H.: Intra-crystalline protein diagenesis (IcPD) in Patella vulgata. Part II: Breakdown and temperature sensitivity, Quat. Geochronol., 16, 158–172, https://doi.org/10.1016/j.quageo.2012.08.001, 2013a.

Demarchi, B., Rogers, K., Fa, D. A., Finlayson, C. J., Milner, N., and Penkman, K. E. H.: Intra-crystalline protein diagenesis (IcPD) in Patella vulgata. Part I: Isolation and testing of the closed system, Quat. Geochronol., 16, 144–157, https://doi.org/10.1016/j.quageo.2012.03.016, 2013b.

Demarchi, B., Clements, E., Coltorti, M., van de Locht, R., Kröger, R., Penkman, K., and Rose, J.: Testing the effect of bleaching on the bivalve Glycymeris: A case study of amino acid geochronology on key Mediterranean raised beach deposits, Quat. Geochronol., 25, 49–65, https://doi.org/10.1016/j.quageo.2014.09.003, 2015.

Dickinson, M. R., Lister, A. M., and Penkman, K. E. H.: A new method for enamel amino acid racemization dating: A closed system approach, Quat. Geochronol., 50, 29–46, https://doi.org/10.1016/j.quageo.2018.11.005, 2019.

Dominguez, J. G., Kosnik, M. A., Allen, A. P., Hua, Q., Jacob, D. E., Kaufman, D. S., and Whitacre, K.: Time-averaging and stratigraphic resolution in death assemblages and Holocene deposits, PALAIOS, 31, 564–575, https://doi.org/10.2110/palo.2015.087, 2016.

Dunca, E., Mutvei, H., Göransson, P., Mörth, C. M., Schöne, B. R., Whitehouse, M. J., Elfman, M., and Baden, S. P.: Using ocean quahog (Arctica islandica) shells to reconstruct palaeoenvironment in Öresund, Kattegat and Skagerrak, Sweden. Int. J. Earth Sci., 98, 3–17, https://doi.org/10.1007/s00531-008-0348-6, 2009.

Estrella-Martínez, J.: Holocene climate variability in UK waters based on Arctica islandica sclerochronology, PhD thesis, Bangor University, 2019.

Estrella-Martínez, J., Ascough, P. L., Schöne, B. R., Scourse, J. D., and Butler, P. G.: 8.2 ka event North Sea hydrography determined by bivalve shell stable isotope geochemistry, Sci. Rep., 9, 1–9, https://doi.org/10.1038/s41598-019-43219-1, 2019.

Eyles, N., McCabe, A. M., and Bowen, D. Q.: The stratigraphic and sedimentological significance of Late Devensian ice sheet surging in Holderness, Yorkshire, Quaternary Sci. Rev., 13, 727–759, https://doi.org/10.1016/0277-3791(94)90102-3, 1994.

Goodfriend, G. A., Hare, P. E., and Druffel, E. R. M.: Aspartic acid racemization and protein diagenesis in corals over the last 350 years Geochim. Cosmochim. Ac., 56, 3847–3850, https://doi.org/10.1016/0016-7037(94)00324-F, 1992.

Goodfriend, G. A. and Weidman, C. R.: Ontogenetic trends in aspartic acid racemization and amino acid composition within modern and fossil shells of the bivalve Arctica, Geochim. Cosmochim. Ac., 65, 1921–1932, https://doi.org/10.1016/S0016-7037(01)00564-6, 2001.

Goodfriend, G. A., Kashgarian, M., and Harasewych, M. G.: Use of aspartic acid racemization and post-bomb 14C to reconstruct growth rate and longevity of the deep-water slit shell Entemnotrochus adansonianus, Geochim. Cosmochim. Ac., 59, 1125–1129, https://doi.org/10.1016/0016-7037(95)00029-Y, 1995.

Goodfriend, G. A., Flessa, K. W., and Hare, P. E.: Variation in amino acid epimerization rates and amino acid composition among shell layers in the bivalve Chione from the Gulf of California, Geochim. Cosmochim. Ac., 61, 1487–1493, 1997.

Gries, K., Kröger, R., Kübel, C., Fritz, M., and Rosenauer, A.: Investigations of voids in the aragonite platelets of nacre, Acta Biomater., 5, 3038–3044, https://doi.org/10.1016/j.actbio.2009.04.017, 2009.

Hajdas, I., Ascough, P., Garnett, M. H., Fallon, S. J., Pearson, C. L., Quarta, G., Spalding, K. L., Yamaguchi, H., and Yoneda, M.: Radiocarbon dating, Nat. Rev. Methods Primers, 1, 62, https://doi.org/10.1038/s43586-021-00058-7, 2021.

Hamblin, R. J. O., Moorlock, B. S. P., Booth, S. J., Jeffery, D. H., and Morigi, A. N.: The Red Crag and Norwich Crag formations in eastern Suffolk, Proc. Geol. Assoc., 108, 11–23, https://doi.org/10.1016/S0016-7878(97)80002-8, 1997.

Hare, P. E. and Mitterer, R. M.: Laboratory simulation of amino acid diagenesis in fossils, Carnegie Inst. Wash. YRB, 67, 205–208, 1969.

Haugen, J.-E. and Sejrup, H. P.: Amino acid composition of aragonitic concholin in the shell of Arctica islandica, Lethaia, 23, 133–141, https://doi.org/10.1111/j.1502-3931.1990.tb01354.x, 1990.

Haugen, J. E. and Sejrup, H. P.: Isoleucine epimerization kinetics in the shell of Arctica islandica, Norsk Geologisk Tidsskrift, 72, 171–180, 1992.

Hendy, E. J., Tomiak, P. J., Collins, M. J., Hellstrom, J., Tudhope, A. W., Lough, J. M., and Penkman, K. E. H.: Assessing amino acid racemization variability in coral intra-crystalline protein for geochronological applications, Geochim. Cosmochim. Ac., 86, 338–353, https://doi.org/10.1016/j.gca.2012.02.020, 2012.

Huang, Q., Agbaje, O. B. A., Conti, M., and Schöne, B. R.: Organic phases in bivalve (Arctica islandica) shells: Their bulk and amino acid nitrogen stable isotope compositions, Geochem. Geophys. Geosyst., 24, e2023GC011147, https://doi.org/10.1029/2023GC011147, 2023.

IUGS: International Chronostratigraphic Chart, v 2023/09, https://stratigraphy.org/chart (last access: 24 February 2024), 2023.

Kaufman, D. S., Cooper, K., Behl, R., Billups, K., Bright, J., Gardner, K., Hearty, P., Jakobsson, M., Mendes, I., O'Leary, M., Polyak, L., Rasmussen T., Rosa, F., and Schmidt, M.: Amino acid racemization in mono-specific foraminifera from Quaternary deep-sea sediments, Quat. Geochronol., 16, 50–61, https://doi.org/10.1016/j.quageo.2012.07.006, 2013.

Kosnik, M. A. and Kaufman, D. S.: Identifying outliers and assessing the accuracy of amino acid racemization measurements for geochronology: II. Data screening, Quat. Geochronol., 3, 328–341, https://doi.org/10.1016/j.quageo.2008.04.001, 2008.

Kriausakul, N. and Mitterer, R. M.: Isoleucine epimerization in peptides and proteins: kinetic factors and application to fossil proteins, Science, 201, 1011–1014, https://doi.org/10.1126/science.201.4360.1011, 1978.

Malatesta, A. and Zarlenga, F.: Northern guests in the Pleistocene Mediterranean Sea, Geologica Romana, 25, 91–154, 1986.

Marchitto, T. M., Jones, G. A., Goodfriend, G. A., and Weidman, C. R.: Precise temporal correlation of Holocene mollusk shells using sclerochronology, Quaternary Res., 53, 236–246, https://doi.org/10.1006/qres.1999.2107, 2000.

Mayhew, D. F.: West European arvicolid evidence of intercontinental connections during the Early Pleistocene, Quaternary Int., 284, 62–73, https://doi.org/10.1016/j.quaint.2011.08.005, 2013.

Milano, S., Nehrke, G., Wanamaker Jr., A. D., Ballesta-Artero, I., Brey, T., and Schöne, B. R.: The effects of environment on Arctica islandica shell formation and architecture, Biogeosciences, 14, 1577–1591, https://doi.org/10.5194/bg-14-1577-2017, 2017.

Millman, E., Wheeler, L., Billups, K., Kaufman, D., and Penkman, K. E. H.: Testing the effect of oxidizing pre-treatments on amino acids in benthic and planktic foraminifera tests, Quat. Geochronol., 73, 101401, https://doi.org/10.1016/j.quageo.2022.101401, 2022.

NOAA: Index of /pub/data/paleo/aar, NOAA [data set], https://www.ncei.noaa.gov/pub/data/paleo/aar/, last access: 9 May 2024.

Orem, C. A. and Kaufman, D. S.: Effects of basic pH on amino acid racemization and leaching in freshwater mollusk shell, Quat. Geochronol., 6, 233–245, https://doi.org/10.1016/j.quageo.2010.11.005, 2011.

Ortiz, J. E., Torres, T., González-Morales, M. R., Abad, J., Arribas, I., Fortea, F. J., Garcia-Belenguer, F., and Gutiérrez-Zugasti, I.: The aminochronology of man-induced shell middens in caves in Northern Spain, Archaeometry, 51, 123–139, https://doi.org/10.1111/j.1475-4754.2008.00383.x, 2009.

Ortiz, J. E., Torres, T., and Pérez-González, A.: Amino acid racemization in four species of ostracodes: Taxonomic, environmental, and microstructural controls, Quat. Geochronol., 16, 129–143, https://doi.org/10.1016/j.quageo.2012.11.004, 2013.

Ortiz, J. E., Gutiérrez-Zugasti, I., Torres, T., González-Morales, M., and Sánchez-Palencia, Y.: Protein diagenesis in Patella shells: Implications for amino acid racemisation dating, Quat. Geochronol., 27, 105–118, https://doi.org/10.1016/j.quageo.2015.02.008, 2015.

Ortiz, J. E., Sánchez-Palencia, Y., Gutiérrez-Zugasti, I., Torres, T., and González-Morales, M.: Protein diagenesis in

archaeological gastropod shells and the suitability of this material for amino acid racemisation dating: Phorcus lineatus (da Costa, 1778), Quat. Geochronol., 46, 16–27, https://doi.org/10.1016/j.quageo.2018.02.002, 2018.

Penkman, K.: Amino acid geochronology: Its impact on our understanding of the Quaternary stratigraphy of the British Isles, J. Quat. Sci., 25, 501–514, https://doi.org/10.1002/jqs.1346, 2010.

Penkman, K. E. H. and Wenban-Smith, F.: Amino acid dating, in: The Ebbsfleet elephant: Excavations at Southfleet Road, Swanscombe in advance of High Speed 1, 2003-4, edited by: Wenban-Smith, F., Oxford Archaeology, 20, 307–318, 2013.

Penkman, K. E. H., Preece, R. C., Keen, D. H., Maddy, D., Schreve, D. C., and Collins, M. J.: Testing the aminostratigraphy of fluvial archives: the evidence from intra-crystalline proteins within freshwater shells, Quat. Sci. Rev., 26, 2958–2969, https://doi.org/10.1016/j.quascirev.2007.06.034, 2007.

Penkman, K. E. H., Kaufman, D. S., Maddy, D., and Collins, M. J.: Closed-system behaviour of the intra-crystalline fraction of amino acids in mollusc shells, Quat. Geochronol., 3, 2–25, https://doi.org/10.1016/j.quageo.2007.07.001, 2008.

Poulsen, B.: Dutch Herring – An Environmental History, c. 1600–1860, Amsterdam University, 2008.

Preece, R. C. and Penkman, K. E. H.: New faunal analyses and amino acid dating of the Lower Palaeolithic site at East Farm, Barnham, Suffolk. Proc. Geol. Assoc., 116, 363–377, https://doi.org/10.1016/S0016-7878(05)80053-7, 2005.

Preece, R. C., Meijer, T., Penkman, K. E. H., Demarchi, B., Mayhew, D. F., and Parfitt, S. A.: The palaeontology and dating of the 'Weybourne Crag', an important marker horizon in the Early Pleistocene of the southern North Sea basin, Quat. Sci. Rev., 236, 106177, https://doi.org/10.1016/j.quascirev.2020.106177, 2020.

Reichert, K. L., Licciardi, J. M., and Kaufman, D. S.: Amino acid racemization in lacustrine ostracodes, part II: Paleothermometry in Pleistocene sediments at Summer Lake, Oregon, Quat. Geochronol., 6, 174–182, https://doi.org/10.1016/j.quageo.2010.11.007, 2011.

Reynolds, D. J., Scourse, J. D., Halloran, P. R., Nederbragt, A. J., Wanamaker, A. D., Butler, P. G., Richardson, C. A., Heinemeier, J., Eiríksson, J., Knudsen, K. L., and Hall, I. R.: Annually resolved North Atlantic marine climate over the last millennium, Nat. Commun., 7, 201–217, https://doi.org/10.1038/ncomms13502, 2016.

Ryan, D. D., Lachlan T. J., Murray-Wallace, C. V., and Price, D. M.: The utility of single foraminifera amino acid racemization analysis for the relative dating of Quaternary beach barriers and identification of reworked sediment, Quat. Geochronol., 60, 101103, https://doi.org/10.1016/j.quageo.2020.101103, 2020.

Schöne, B. R.: Arctica islandica (Bivalvia): A unique paleoenvironmental archive of the northern North Atlantic Ocean, Global Planet. Change, 111, 199–225, https://doi.org/10.1016/j.gloplacha.2013.09.013, 2013.

Schöne, B. R. and Fiebig, J.: Seasonality in the North Sea during the Allerød and Late Medieval Climate Optimum using bivalve sclerochronology, Int. J. Earth Sci., 98, 83–98, https://doi.org/10.1007/s00531-008-0363-7, 2009.

Schöne, B. R. and Huang, Q.: Ontogenetic $\delta$15N Trends and Multidecadal Variability in Shells of the Bivalve Mollusk, Arctica islandica, Front. Mar. Sci., 8, 1–15, https://doi.org/10.3389/fmars.2021.748593, 2021.

Schöne, B. R., Freyre Castro, A. D., Fiebig, J., Houk, S. D., Oschmann, W., and Kröncke, I.: Sea surface water temperatures over the period 1884-1983 reconstructed from oxygen isotope ratios of a bivalve mollusk shell (Arctica islandica, southern North Sea), Palaeogeogr. Palaeocl., 212, 215–232, https://doi.org/10.1016/j.palaeo.2004.05.024, 2004.

Schöne, B. R., Fiebig, J., Pfeiffer, M., Gleß, R., Hickson, J., Johnson, A. L. A., Dreyer, W., and Oschmann, W.: Climate records from a bivalved Methuselah (Arctica islandica, Mollusca; Iceland), Palaeogeogr. Palaeocl., 228, 130–148, https://doi.org/10.1016/j.palaeo.2005.03.049, 2005.

Scourse, J. D., Afrifa, K., Byrne, L., Crowley, D., Earland, J. L., Ehmen, T., Frøslev, T. G., Greenall, C., Harland, J., Heard, Z., Höche, N., Holman, L. E., Huang, Q., Langkjær, E. M. R., Mason, M., Nelson, E., Nemeth, Z., Reynolds, D., Robson, H. K., Roman-Gonzalez, A., Scherer, P., Scolding, J., Short, J., Wilkin, J. T. R., and Wilson, D. R.: DY150 Cruise report, https://seachange-erc.eu/research/north-west-european-research-cruise (last access: 20 February 2024), 2022.

Sejrup, H. P. and Haugen, J. E.: Amino acid diagenesis in the marine bivalve Arctica islandica Linné from northwest European sites: Only time and temperature?, J. Quat. Sci., 9, 301–309, https://doi.org/10.1002/jqs.3390090402, 1994.

Sykes, G. A., Collins, M. J., and Walton, D. I.: The significance of a geochemically isolated intracrystalline organic fraction within biominerals, Org. Geochem., 23, 1059–1065, https://doi.org/10.1016/0146-6380(95)00086-0, 1995.

Tomiak, P. J., Penkman, K. E. H., Hendy, E. J., Demarchi, B., Murrells, S., Davis, S. A., McCullagh, P., and Collins, M. J.: Testing the limitations of artificial protein degradation kinetics using known-age massive Porites coral skeletons, Quat. Geochronol., 16, 87–109, https://doi.org/10.1016/j.quageo.2012.07.001, 2013.

Tomiak, P. J., Andersen, M. B., Hendy, E. J., Potter, E. K., Johnson, K. G., and Penkman, K. E. H.: The role of skeletal micro-architecture in diagenesis and dating of Acropora palmata, Geochim. Cosmochim. Ac., 183, 153–175, https://doi.org/10.1016/j.gca.2016.03.030, 2016.

Torres, T., Ortiz, J. E., and Arribas, I.: Variations in racemization/epimerization ratios and amino acid content of Glycymeris shells in raised marine deposits in the Mediterranean, Quat. Geochronol., 16, 35–49, https://doi.org/10.1016/j.quageo.2012.11.002, 2013.

Towe, K. M. and Thompson, G. R.: The structure of some bivalve shell carbonates prepared by ion-beam thinning – A comparison study, Calcif. Tissue Res., 10, 38–48, 1972.

Trofimova, T., Milano, S., Andersson, C., Bonitz, F. G. W., and Schöne, B. R.: Oxygen isotope composition of Arctica islandica aragonite in the context of shell architectural organization: Implications for paleoclimate reconstructions, Geochem. Geophys. Geosyst., 19, 453–470, https://doi.org/10.1002/2017GC007239, 2018.

Vallentyne, J. R.: Biogeochemistry of organic matter II: Thermal reaction kinetics and transformation products of amino compounds, Geochim. Cosmochim. Ac., 28, 157–188, 1964.

Walker, M., Head, M. J., Lowe, J., Berkelhammer, M., Björck, S., Cheng, H., Cwynar, L. C., Fisher, D., Gkinis, V., Long, A., Newnham, R., Rasmussen, S. O., and Weiss, H.: Subdividing the Holocene Series/Epoch: formalization

of stages/ages and subseries/subepochs, and designation of GSSPs and auxiliary stratotypes, J. Quat. Sci., 34, 173–186, https://doi.org/10.1002/jqs.3097, 2019.

Walton, D.: Degradation of intracrystalline proteins and amino acids in fossil brachiopods, Org. Geochem., 28, 389–410, 1998.

Wanamaker Jr., A. D., Butler, P. G., Scourse, J. D., Heinemeier, J., Eiríksson, J., Knudsen, K. L., and Richardson, C. A.: Surface changes in the North Atlantic meridional overturning circulation during the last millennium, Nat. Commun., 3, 1–7, https://doi.org/10.1038/ncomms1901, 2012.

Wheeler, L. J., Penkman, K. E. H., and Sejrup, H. P.: Assessing the intra-crystalline approach to amino acid geochronology of Neogloboquadrina pachyderma (sinistral), Quat. Geochronol., 61, 101131, https://doi.org/10.1016/j.quageo.2020.101131, 2021.

Witbaard, R., Duineveld, G. C. A., and de Wilde, P. A. W. J.: A long-term growth record derived from Arctica islandica (Mollusca, Bivalvia) from the Fladen ground (northern North Sea), J. Mar. Biol. Assoc. UK, 77, 801–816, https://doi.org/10.1017/s0025315400036201, 1997.